THE BDM CORPORATION
1801 RANDOLPH ROAD, S.E. · ALBUQUERQUE, NEW MEXICO 87106 · (505) 848-5000

LEVEL II

Evaluation of Spatial Filtering as a Means For Increasing Optical Performance in High Power Beam Trains

WORK PERFORMED FOR DARPA/AFWL
UNDER CONTRACT MDA-903-80-C-0339

SEPTEMBER 16, 1981

BDM/A-81-605-TR

THE BDM CORPORATION
1801 RANDOLPH ROAD, S.E. · ALBUQUERQUE, NEW MEXICO 87106 · (505) 848-5000 · TWX 910-989-0619

(14) BDM/A-81-605-TR

(9) Final technical rept.

(6) EVALUATION OF SPATIAL FILTERING AS A MEANS FOR INCREASING OPTICAL PERFORMANCE IN HIGH POWER BEAM TRAINS.

(11) 16 Sept [redacted] 81

(12) 76

WORK PERFORMED FOR DARPA/AFWL
UNDER CONTRACT (15) MDA 903-80-C-0339, DARPA Order C-0071

CONTRIBUTORS:

(10) Carl Wiggins
Dr. George Lawrence
Dr. Lyn Skolnik
John Corcoran

Accession For	
NTIS GRA&I	X
DTIC TAB	☐
Unannounced	☐
Justification	
By Per Ltr. on File	
Distribution/	
Availability Codes	
Dist	Avail and/or Special
A	

JOS

FOREWORD

This final technical report, BDM/A-81-605-TR, is submitted by The BDM Corporation, 1801 Randolph Road S.E., Albuquerque, New Mexico 87106 in accordance with the requirements for DARPA Task Order number C-007 entitled "Spatial Filter Study," under contract number MDA-903-80-C-0339.

The DARPA subtask officer is Colonel Ronald F. Prater (DARPA/DEO). The technical monitor on this subtask is Dr. Russ Butts (AFWL/ARAA).

This report consists of annotated vugraphs covering objectives of the subtask statement. The major results on the effectiveness of spatial filtering on highly nonuniform intensity distributions in high power laser beam trains should be of general interest to the optics community at large and will, upon proper authorization, be submitted for journal publication in the open literature.

PROBLEM STATEMENT

The intensity distribution at the output of a high energy laser (HEL) device can be highly nonuniform. This nonuniform intensity can cause localized thermal distortions in the mirrors in the beam train which, in turn, will induce phase errors on the beam which are also of nonuniform distribution, as illustrated in figure 1. While adaptive optics can in principal correct these phase errors, correction of high spatial frequency errors is beyond the current state of the art of adaptive cooled mirrors.

The basic objective of this study is to investigate the feasibility of using a spatial filter in a HEL beam train to reduce the effects of flux dependent thermal mirror distortions and to improve the far field performance of the optical system.

THE PROBLEM

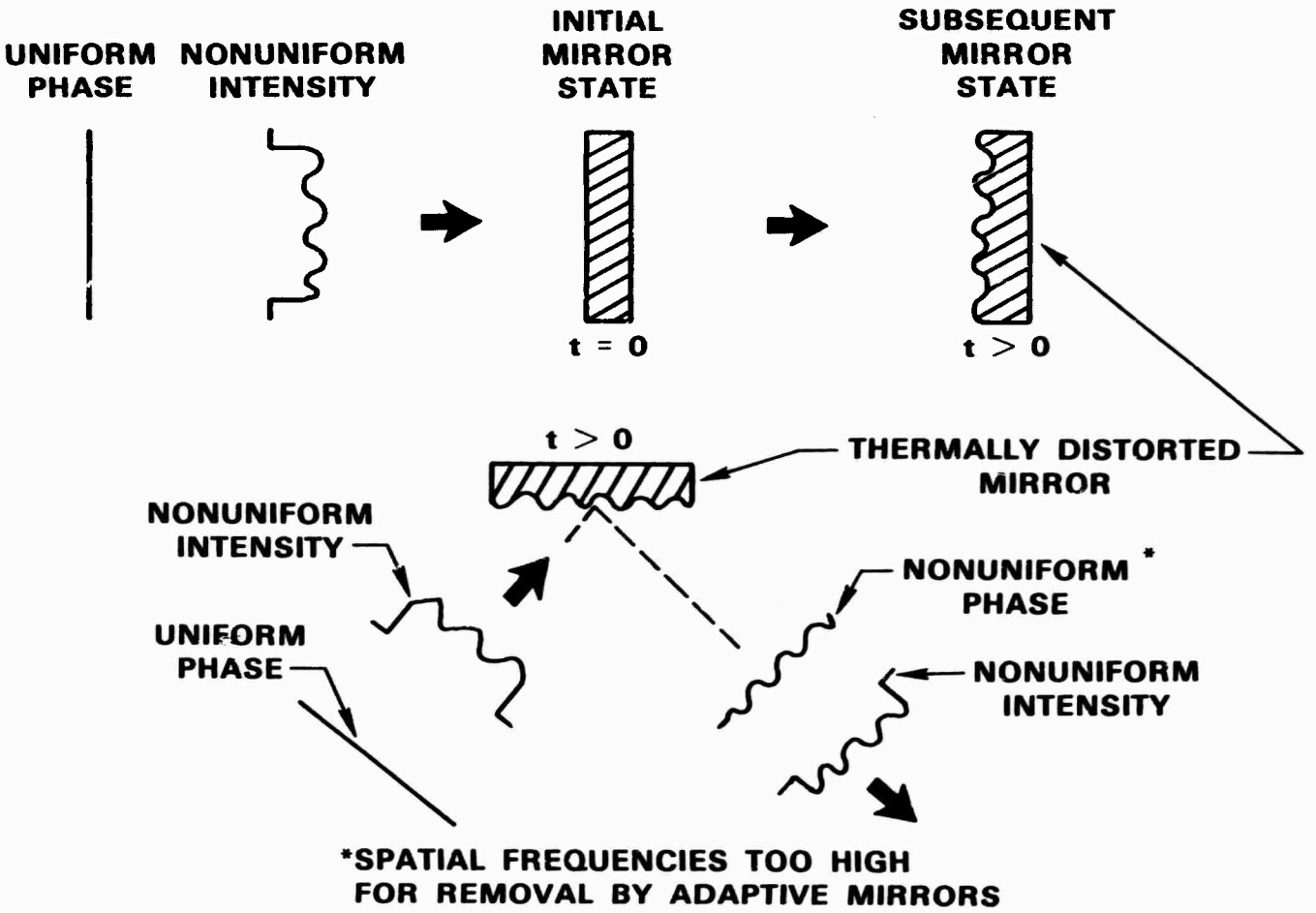

BDM/A-81-606-TR

Figure 1. Illustrating the Problem of Intensity Caused Phase Errors in HEL Optical Systems

APPROACH TO SOLUTION

It is possible that, by including a spatial filter in a HEL beam train, high spatial frequency components of the intensity distribution can be removed. This should result in a beam of more uniform intensity distribution thereby reducing phase errors and mirror thermal distortion. Beam quality should improve thereby increasing the far field intensity.

The concept of a spatial filter is illustrated in figure 2. The spatial filter first focuses the beam (M1) which transforms it from object space to image space (frequency space). In the focal plane of M1 and to the left of P, the spectral distribution of the nonuniform intensity is formed, with higher spatial frequency components occurring at larger transverse distances from the center of the focal plane distribution. The focal plane distribution then passes through a circular aperture of radius "a" at P which removes all frequencies above the cutoff frequency "fc". The remaining spectral distribution to the right of P is then transformed back to pupil space at M2, resulting in the smoothed intensity distribution.

SOLUTION APPROACH — USE A SPATIAL FILTER TO REMOVE HIGH FREQUENCIES

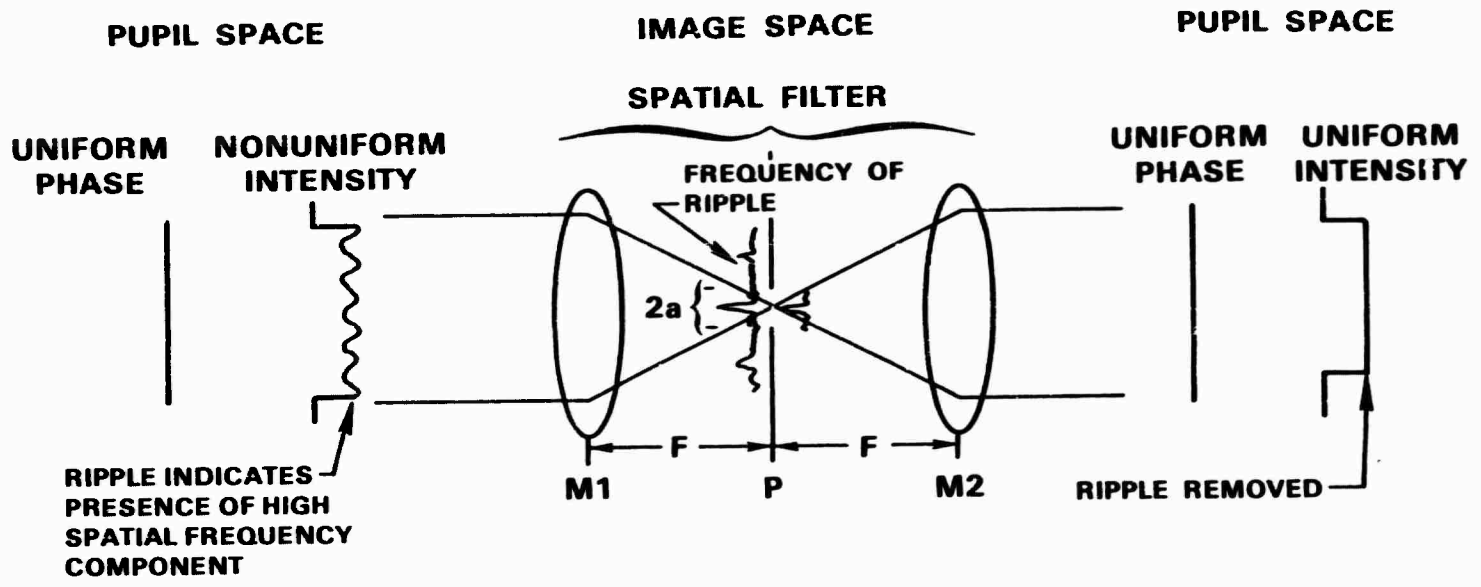

SPATIAL FILTER OF RADIUS a REMOVES ALL SPATIAL FREQUENCIES ABOVE CUT OFF FREQUENCY

$$fc = \frac{a}{\lambda F}$$

BDM/A-81-605-TR

Figure 2. Illustrating the Concept of a Spatial Filter

There are four detailed objectives of this study (figure 3). The first objective requires building computer models characterizing: (1) the initial nonuniform intensity distributions of a HEL device; (2) a representative HEL beam train with spatial filter and flux dependent thermal distortion models; and (3) the measures of far field performance. Also included in the first objectve is the determination of how much phase error is produced by the nonuniform flux loads on the mirrors in the beam train in the absence of spatial filtering and what far field performance level results. This is the baseline response of the beam train. The second objective requires placing a spatial filter at locations in the beam train, varying its radius (cutoff frequency), and comparing the resulting level of optical performance to baseline (no filter) performance. The third objective involves analyzing the geometrical aspects of filter design to minimize the flux loads on the filter. The last objective then addresses filter design from the standpoint of best material selection.

OBJECTIVES

1) MODEL THERMAL PROPERTIES OF A HEL BEAM TRAIN AND DETERMINE IMPACT OF NONUNIFORM INTENSITY DISTRIBUTION ON MIRROR DISTORTION AND FAR FIELD PERFORMANCE

2) ASSESS USEFULNESS OF SPATIAL FILTERING FOR REDUCING THERMALLY INDUCED BEAM TRAIN ABERRATION

3) CONCEPTUAL DESIGN OF BEAM TRAIN INCLUDING SPATIAL FILTER AND PROBLEMS CAUSED

4) FIND BEST MATERIAL AND DESIGN FOR SPATIAL FILTER

Figure 3. The Study Objectives

The fundamental conclusion reached as a result of this study is that spatial filtering of highly nonuniform intensity distributions, particularly those characterized by truncated Gaussians with central and radial obscurations, actually decreases far field performance. This is true whether or not additional high spatial frequency components (originating in the device) are present in the distribution. This result, to be discussed in detail shortly, is believed to be intrinsically related to the naturally high frequency components of large spectral amplitude which characterize sharp-edged intensity distributions.

CONCLUSION

SPATIAL FILTERING OF A HIGHLY NON UNIFORM INTENSITY DISTRIBUTION DOES NOT RESULT IN INCREASED FAR FIELD PERFORMANCE: STREHL, PEAK FAR FIELD INTENSITY, AND POWER INSIDE AN AIRY SPOT ALL DECREASE WITH INCREASING AMOUNTS OF SPATIAL FILTERING WHILE POWER LOSS TO THE FILTER INCREASES.

Figure 4. Fundamental Conclusion of the Study

THE BDM CORPORATION

SUMMARY OF RESULTS

The effect of spatial filtering a truncated Gaussian beam with central and radial obscurations and with a 10 percent peak amplitude modulated sinusoidal component of 1.84 cm period added to the intensity distribution is summarized in figure 5. Performance with the spatial filter is compared to performance without it (baseline). (The model used to calculate the results presented here will be described subsequently.) Optical performance is measured in four ways: peak intensity in the far field; strehl ratio at the primary mirror of the beam train; the amount of power focusable inside a spot of specified size (e.g., the central Airy disk); and the power removed from the beam by the spatial filter. Performance at two different spatial filter radii (i.e. cutoff frequencies) is shown. A filter radius of .029 cm just removes the center of the added 0.544 cycle/cm component and results in significant decrease in the performance relative to baseline. At a radius of .002 cm the filter has so dramatically reduced the spectral distribution that the resulting profile is now Gaussian instead of obscurated-Gaussian. While this results in a 13 percent improvement in strehl ratio, all other performance measures are substantially worsened; peak far field intensity down by 31 percent, power in bucket down 7 percent, and power clipped by filter is up 39 percent.

OVERALL PERFORMANCE DEGRADES WITH INCREASING AMOUNTS OF SPATIAL FILTERING

TRUNCATED, OBSCURED GAUSSIAN WITH 1.84 cm INTENSITY RIPPLE
(USING MODEL A)

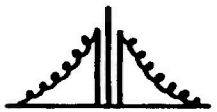

	MEASURE OF PERFORMANCE			
	RELATIVE PEAK INTENSITY	STREHL	RELATIVE POWER IN AIRY SPOT	POWER LOSS TO FILTER (%)
WITHOUT SPATIAL FILTER (BASELINE)	1.0	.87007	1.0	0.0
WITH SPATIAL FILTER				
r = .029 cm[1]	0.88	.86277	0.86	3.0
(% CHANGE)	(-12%)	(-.8%)	(-14.5%)	
r = .002 cm[2]	0.69	.98509	0.93	39.0
(% CHANGE)	(-31.4%)	(+13.2%)	(-7.3%)	

(1) FILTER JUST CLIPPING ADDED RIPPLE FREQUENCY

(2) FILTER SETTING FOR BEST COMBINED FOCUSED POWER AND STREHL

BDM/A-81-605-TR

Figure 5. Summary of Results of the Effect of Spatial Filtering on Truncated, Obscured Gaussian Beams.

Optical performance as a function of spatial filter cutoff frequency is shown in figure 6 for a 10-mirror HEL beam train propagating a truncated Gaussian with central and radial obscurations and with a 0.544 cycle/cm spatial frequency component added. Peak intensity, strehl and power in a bucket the size of the central Airy disk are normalized by their baseline values and plotted on the left abscissa. Baseline values are those at a spatial filter radius sufficiently great to produce no measurable effect due to filtering and occur for radii of .064 cm and greater. Thus performance increases due to spatial filtering would be denoted by normalized values greater than unity. The power clipped from the beam by the filter is plotted on the right abscissa as a percentage of the total power initially in the beam just prior to filtering. While a slight relative improvement in performance is noted when filtering near the center of the added frequency component (.0294 cm in image plane), there is, overall, a decrease in performance with increasing amounts of spatial filtering (smaller filter radii, lower cutoff frequency). At very small filter radii there is a tendency toward improvement (peaking of power in bucket at .002 cm), but baseline performance is never equalled or surpassed.

OPTICAL PERFORMANCE VS. SPATIAL FILTER RADIUS (i.e., PERFORMANCE VS. CUTOFF FREQUENCY) (MODEL A)

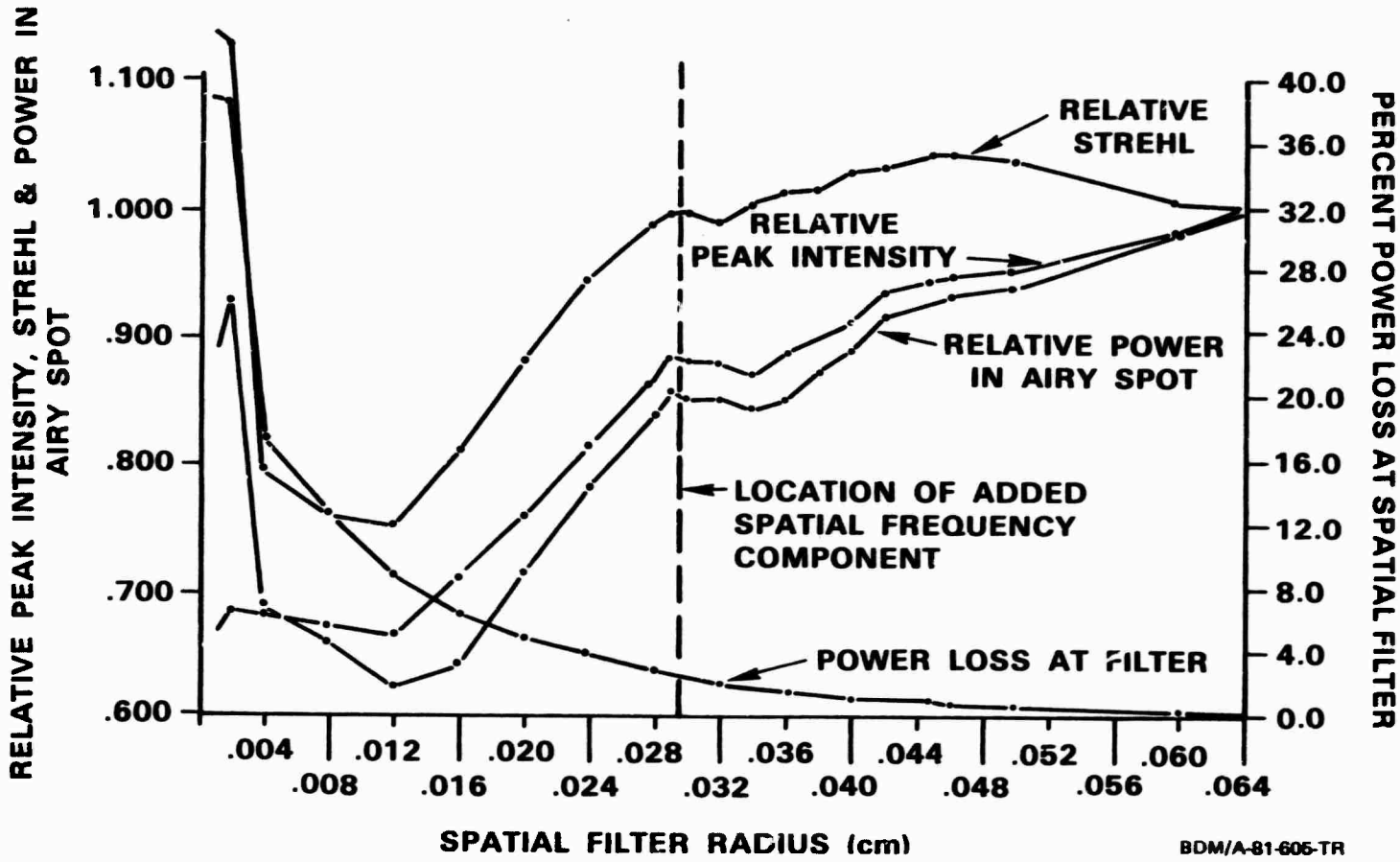

Figure 6. Relative Effectiveness of Spatial Filtering for Increasing the Performance of Optical Systems Propagating Truncated Gaussian Beams With Central and Radial Obscurations and Containing a High Spatial Frequency Component (0.544 cycles/cm, Period = 1.84 cm)

EXPLANATION OF SPATIAL FILTERING RESULTS

To understand the effect of spatial filtering on highly nonuniform beams it is instructive first to consider its effect on beams with simpler intensity structure. A beam having a smoother Gaussian intensity profile and a $\frac{1}{e^2}$ radius of ρ can be well described by spatial frequency components below $\frac{1}{\rho}$. That is, smooth Gaussian beams are essentially bandlimited in terms of spatial frequency content. In the image plane (i.e. in spatial frequency space) the location of the nominally highest effective spatial frequency ($\frac{1}{\rho}$) is located at a distance of $\frac{\lambda F}{\rho}$ from the center of the distribution. A sinusoidal intensity component of spatial period (or wavelength) ℓo added to the pupil plane intensity distribution will generate a spatial frequency component $\frac{1}{\ell o}$ in image space centered about a distance $\frac{\lambda F}{\ell o}$ from the center of the distribution. If $\ell o < \rho$, then the spatial frequency $\frac{1}{\ell o}$ is greater than $\frac{1}{\rho}$ and the added sinusoidal component will occur at a greater distance ($\frac{\lambda F}{\ell o} > \frac{\lambda F}{\rho}$) in the plane of the spatial filter. (See figure 7.)

GAUSSIAN LASER BEAMS ARE ESSENTIALLY BANDLIMITED

HIGHEST SPATIAL FREQUENCY ASSOCIATED WITH BEAM SIZE	$= \frac{1}{\rho}$,	WHERE ρ = BEAM RADIUS
LOCATION OF HIGHEST SPATIAL FREQUENCY OF THE BEAM IN THE FOCAL PLANE OF THE FILTER	$= \frac{\lambda F}{\rho}$,	WHERE ρ = WAVELENGTH F = FOCAL LENGTH
SPATIAL FREQUENCY OF AN ADDED COMPONENT	$= \frac{1}{\ell_o}$,	WHERE ℓ_o = SPATIAL PERIOD OF THE COMPONENT
LOCATION OF THE ADDED SPATIAL FREQUENCY COMPONENT IN THE FILTER FOCAL PLANE	$= \frac{\lambda F}{\ell_o}$	

BDM/A-81-606-TR

Figure 7. Definition of Principal Gaussian Beam Parameter Scales in Space (Pupil) and Frequency (Image) Domains

Figure 8 illustrates the definitions given in figure 7. An actual Gaussian laser beam profile A_{ACTUAL} in pupil space and its decomposition into a smooth Gaussian beam A_{IDEAL} plus a sinusoidal noise term ΔA is shown in figure 8.a. As seen, the nominal spatial period ℓo of the noise is less than the nominal beam radius ρ. The first mirror (or lens) of the spatial filter (recall figure 2) transforms A_{ACTUAL} into the frequency domain spectrum of figure 8.b. Here, since the spatial frequency of the noise term is much higher than that of the Gaussian A_{IDEAL}, the two spectral components are well separated and distinct. Note that the transform of A_{IDEAL} is also a Gaussian. Applying a spatial filter of radius r_{SF}, where $\frac{\lambda F}{\rho} < r_{SF} < \frac{\lambda F}{\ell o}$, to the spectral distribution of figure 8.a will pass the frequencies essential to A_{IDEAL} but will remove the noise spectrum. After recollimating the beam at the second mirror (or lens) of the spatial filter (recall figure 2), the resulting pupil space distribution will be A_{IDEAL}. In this example the spatial filter has been used to remove unwanted frequencies above the (essentially limited) bandwidth of the desired intensity distribution.

SPATIAL FILTERING A GAUSSIAN BEAM

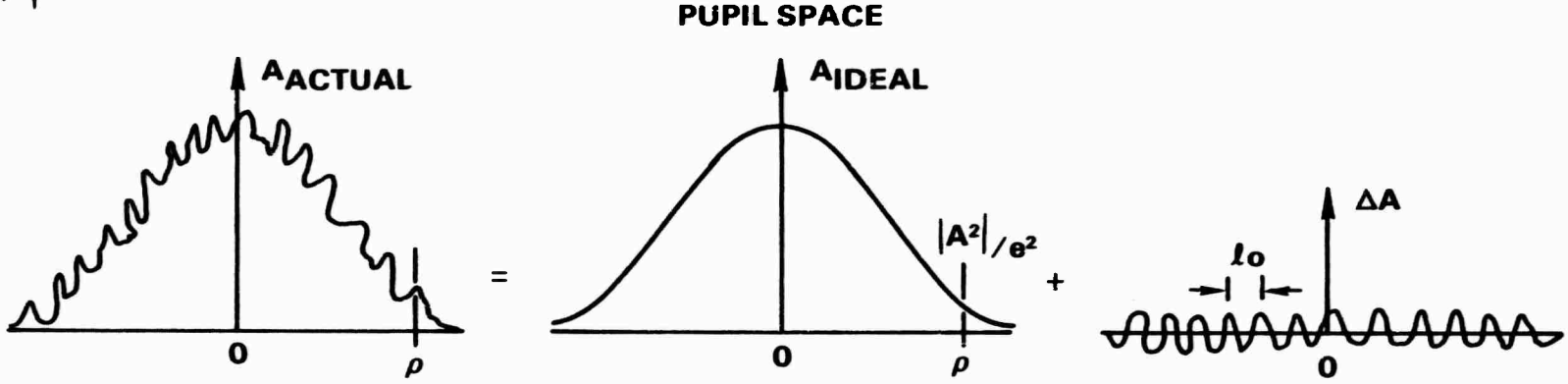

a) SPACE DISTRIBUTION AND DECOMPOSITION

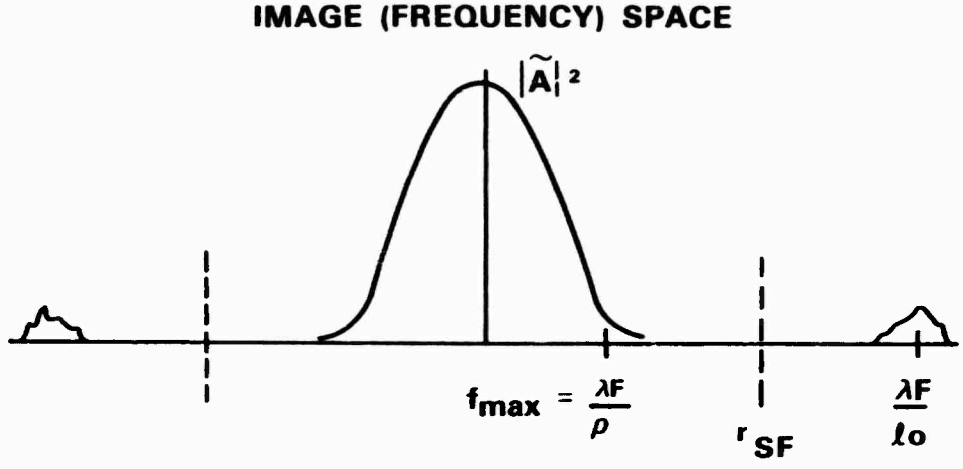

BDM/A-81-605-TR

b) SPATIAL FREQUENCY SPECTRUM

Figure 8. Spatial Filtering a Gaussian Beam to Remove Unwanted Structure

The frequency spectra of two Gaussian beam profiles are shown in figure 9. The solid curve is the transform of a pure Gaussian beam. The dotted curve is the transform of the same Gaussian plus an added 10 percent sinusoidal (ripple) component of ℓo = 1.84 cm spatial period as in figure 8. The center frequency of the added ripple is 0.544 cycle/cm. Since the spectra are symmetric about zero frequency only the positive frequency halves are shown. Spatial frequency is plotted in matrix units (1 matrix unit = .0014063 cm). The center of the added frequency component occurs at 20.87 matrix units or a distance of 0.0294 cm from the center of the spectrum (zero frequency). Taking λ = 2.7μm. F = 200 cm and recalling the definitions given in figure 7, the component at 0.0294 cm corresponds to a spatial frequency of 0.544 cycles/cm. A spatial filter aperture of radius somewhat less than 0.0294 cm would remove this frequency (and any higher ones if present). The resulting spectrum after filtering would be very nearly the same as that of the pure Gaussian, thus the ripple would be removed and there would be very little overall intensity loss.

SPECTRAL DISTRIBUTIONS OF UNTRUNCATED UNOBSCURED GAUSSIANS

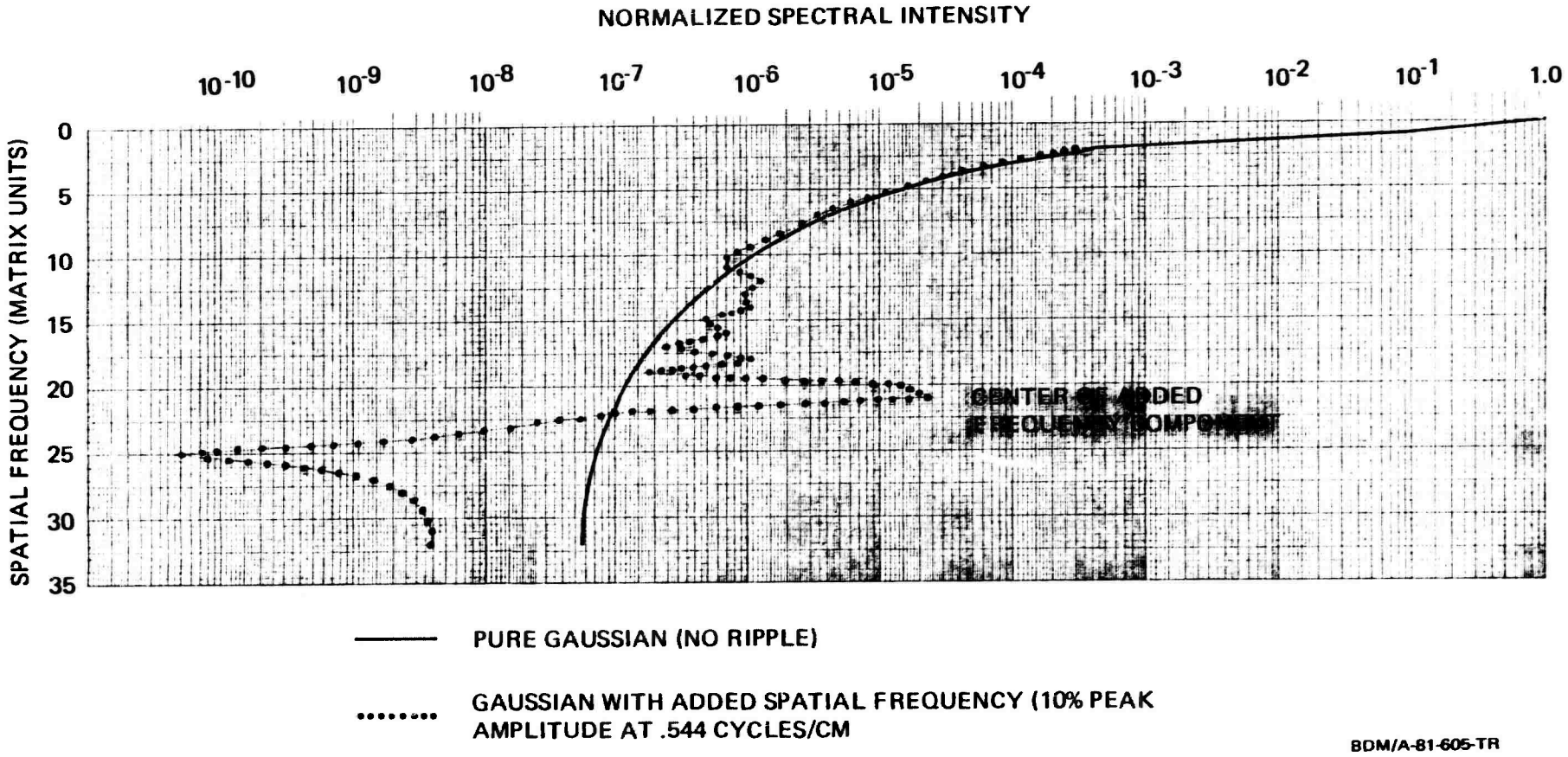

Figure 9. Spectral Distributions of Gaussian Beams With and Without Added 0.544 Cycle/cm Frequency Component

Figure 10 summarizes the effect on overall optical performance of using a spatial filter to remove unwanted spatial frequency of 0.544 cycles/cm from a Gaussian beam. The beam is filtered immediately upon entering the HEL beam train (model A to be discussed presently). The top row elements of figure 10 give the baseline performance, that is, the performance obtained if the spatial filter were not applied (filter radius greater than .064 cm, effectively). Baseline peak intensity in the far field and power in any Airy spot have been arbitrarily normalized to unity. For a filter set to just clip out the center of the added frequency component (r = .0285 cm, second row), the performance has improved slightly relative to baseline. Overall best performance is obtained for a 0.120 cm filter radius, with power in the Airy spot up by 4.6 percent and peak far field intensity increased by 3.4 percent. Thus, for a Gaussian beam profile (no truncations or obscurations), the spatial filter does improve performance as expected.

OVERALL PERFORMANCE IMPROVEMENT WHEN SPATIAL FILTER IS APPLIED TO SMOOTH GAUSSIAN BEAMS WITH ADDED HIGH SPATIAL FREQUENCY (MODEL A)

UNTRUNCATED, UNOBSCURED GAUSSIAN WITH 1.84 cm INTENSITY RIPPLE

	MEASURE OF PERFORMANCE			
	RELATIVE PEAK INTENSITY	STREHL	RELATIVE POWER IN AIRY SPOT	POWER LOSS TO FILTER (%)
WITHOUT SPATIAL FILTER (BASELINE)	1.00	.93827	1.00	0.0
WITH SPATIAL FILTER				
r = .0285 cm[1] (% CHANGE)	1.02 (+1.5%)	.94326 (+0.5%)	1.01 (+1.5%)	0.3
r = .120 cm[2] (% CHANGE)	1.03 (+3.4%)	.95397 (+1.7%)	1.05 (+4.6%)	0.45

(1) FILTER JUST CLIPPING ADDED RIPPLE FREQUENCY

(2) FILTER SETTING FOR BEST PERFORMANCE

BDM/A-81-605-TR

Figure 10. The Effect of Spatial Filtering on Gaussian Beams

Figure 11 shows performance comparisons for two beam profiles, each of which contains the same added spatial frequency component at .544 cycles/cm as a function of spatial filter radius. The performance curves for the truncated, obscured Gaussian beam are the same as in figure 6. The performance curves for the untruncated, unobscured Gaussian beam are seen in the upper portion of the plot. Performance is plotted relative to baseline performance (effectively no filter); parameter values at a filter radius of 0.64 cm are baseline. Except for the percent power clipped by the spatial filter, these parameters have been normalized to unity. Therefore, relative performance greater than unity indicates performance improvement over baseline performance as a result of spatial filtering, and vice versa. As seen, increasing amounts of spatial filtering (i.e. going to smaller filter radii) generally improves performance by essentially a fixed amount and with minor power loss in the case of untruncated, unobscured Gaussian beams, but generally results in increasingly worse performance in the case of truncated, obscured Gaussian beams. The tendency toward improvement at very small filter radii for the truncated, obscured beam is due to the fact that the filter has greatly modified the spectrum until it is nearly Gaussian. But the power loss at the filter is very great, so there is still no net improvement in performance relative to baseline performance.

PERFORMANCE COMPARISONS SHOWING THE EFFECT OF SPATIAL FILTERING ON TWO DIFFERENT BEAMS

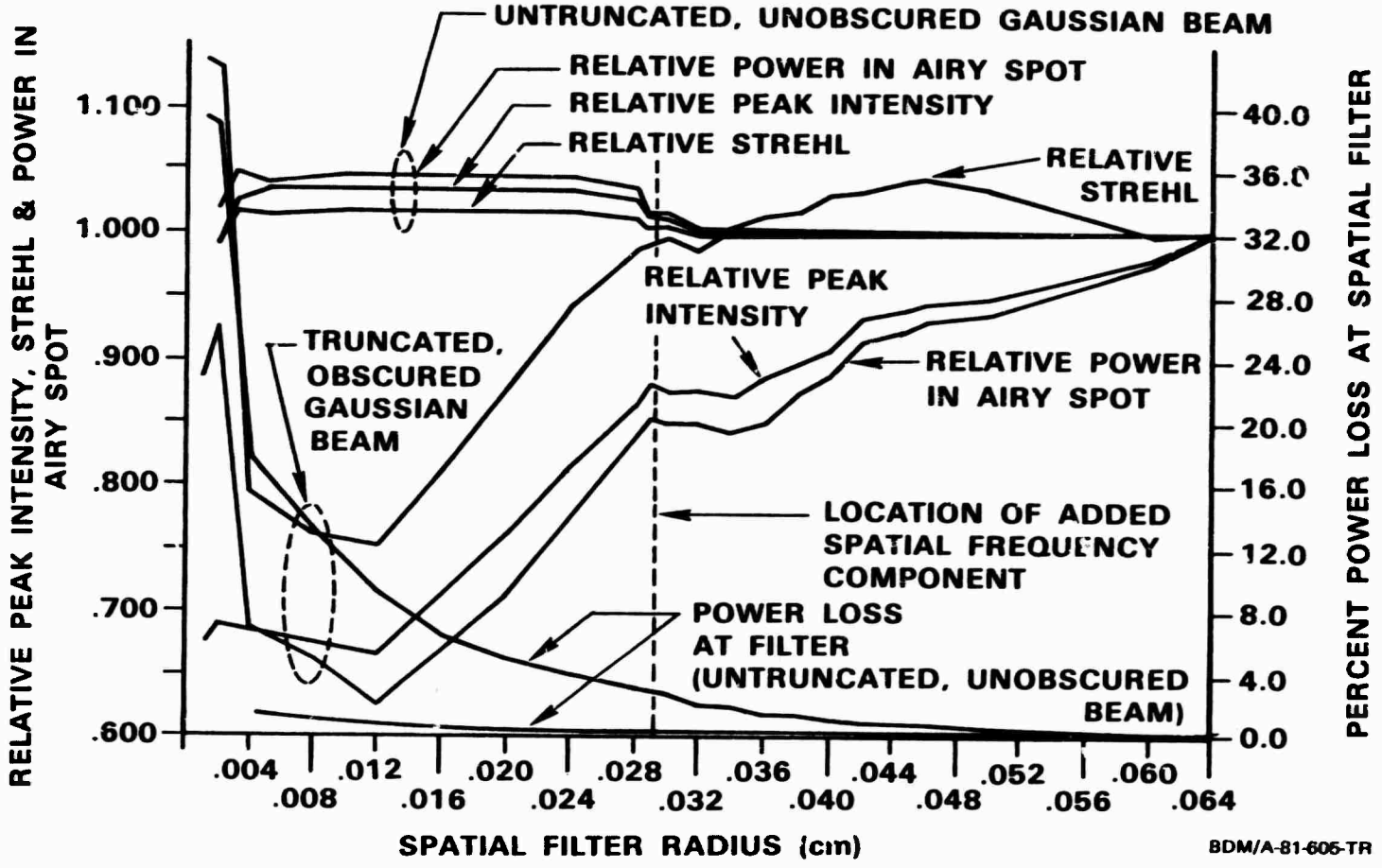

Figure 11. Relative Effectiveness of Spatial Filtering for Increasing the Performance of Optical Systems Propagating Two Different Types of Gaussian Beams Each Containing a High Spatial Frequency Component of Period = 1.84 cm

The two beam profiles show very different performance levels as a function of spatial filtering (figure 11) because their frequency spectra are very different. The frequency distribution (i.e. in the plane of the spatial filter) of the truncated, obscured Gaussian beam is shown in figure 12. There are three important observations to be made: (1) the spectrum is very complex, having many notches and secondary peaks; (2) the spectral amplitude of the envelope of the high frequency structure is several orders of magnitude higher than that of an untruncated, unobscured Gaussian beam (compare figure 12 with figure 9); and (3) the addition of a 10 percent ripple component of 1.84 cm period to the space distribution (.544 cycle/cm) has only a relatively minor effect on the spectrum (dotted curve vs. solid curve). The presence of higher amplitude, high frequency components in the basic beam spectrum means that spatial filtering will have a pronounced effect since it will truncate the spectrum: the basic beam shape will be significantly modified even at relatively large filter radii.

SPECTRAL DISTRIBUTION OF A HIGHLY NONUNIFORM BEAM PROFILE: TRUNCATED GAUSSIAN WITH RADIAL AND CENTRAL OBSCURATIONS

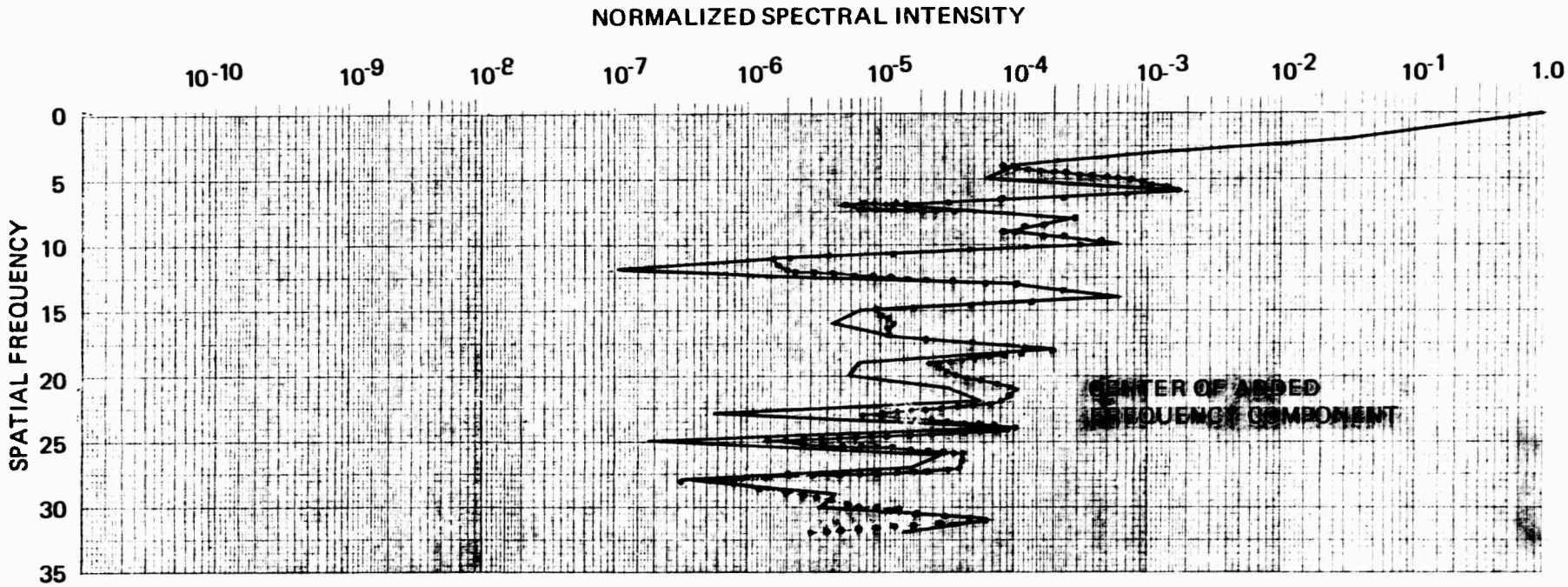

——— FREQUENCY SPECTRUM WITH NO ADDED SPATIAL FREQUENCY COMPONENT

..... FREQUENCY SPECTRUM WITH 0.544 CYCLES/CM COMPONENT ADDED AT 10% MODULATION

BDM/A-81-605-TR

Figure 12. The Spectral Distributions of Truncated Obscured Gaussian Beams With and Without a 0.544 Cycle/cm Component Added

The effect of the spatial filter on the two beam profiles is very different. In the case of the untruncated, unobscured Gaussian beam, there is very little spectral amplitude at .544 cycles/cm (solid curve, figure 9) until the .544 cycle/cm component has been added (dotted curve, figure 9). Therefore, application of the spatial filter removes only the unwanted frequency. As a result, there is no significant change in the shape of the beam profile or its phase. In the case of the truncated, obscured Gussian beam, there is already significant spectral amplitude at .544 cycles/cm and beyond (solid curve, figure 12) before the .544 cycle/cm component is added (dotted curve, figure 12). Therefore, application of the spatial filter removes desirable frequency components in addition to the unwanted frequency. Not only is the basic beam profile modified significantly (smoothed curves) and relatively larger amounts of power removed by filtering, but there is a corresponding significant change in the phase of the beam. These basic results are summarized in figure 13.

COMPARISON OF SPATIAL FILTER EFFECT ON TWO DIFFERENT BEAM SHAPES

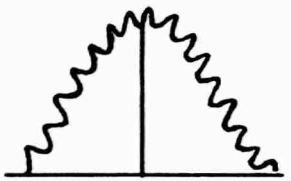

SMOOTH, UNOBSCURED, UNTRUNCATED GAUSSIAN CONTAINS VERY LITTLE HIGH FREQUENCY EXCLUSIVE OF THE ADDED COMPONENT SO SPATIAL FILTER HAS LITTLE EFFECT ON THE DOMINANT BEAM SHAPE

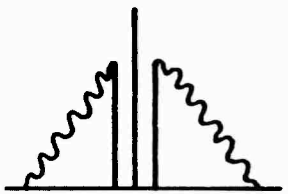

OBSCURED, TRUNCATED GAUSSIAN CONTAINS FREQUENCY COMPONENTS AT FREQUENCIES MUCH HIGHER THAN THAT OF THE ADDED COMPONENT SO SPATIAL FILTER WILL SIGNIFICANTLY ALTER THE DOMINANT BEAM SHAPE AND THE PHASE.

BDM/A-81-605-TR

Figure 13. Comparison of Spatial Filter Effects for Two Different Beam Profiles

TRUNCATED, OBSCURED GAUSSIAN BEAMS ARE NOT BANDLIMITED

A truncated, obscured Gaussian intensity distribution typically describes the HEL intensity distribution. Because of the sharp edges near the truncations and obscurations, the spatial frequency spectrum is not bandlimited; the spectrum contains essentially all frequencies. This is true whether or not there are additional high spatial frequencies present (caused by the HEL device). The effect of the spatial filter on such a beam is to remove higher spatial frequencies (above filter cutoff). This smooths the distribution by rounding off the sharp corners, but also modifies the phase as seen, making it less focusable. Figure 14 shows the beam profiles (intensity and phase) immediately before and after applying the spatial filter. The net effect of the filter is to reduce the amount of energy in the beam and make it harder to focus. This causes the overall decrease in performance with increasing spatial filtering.

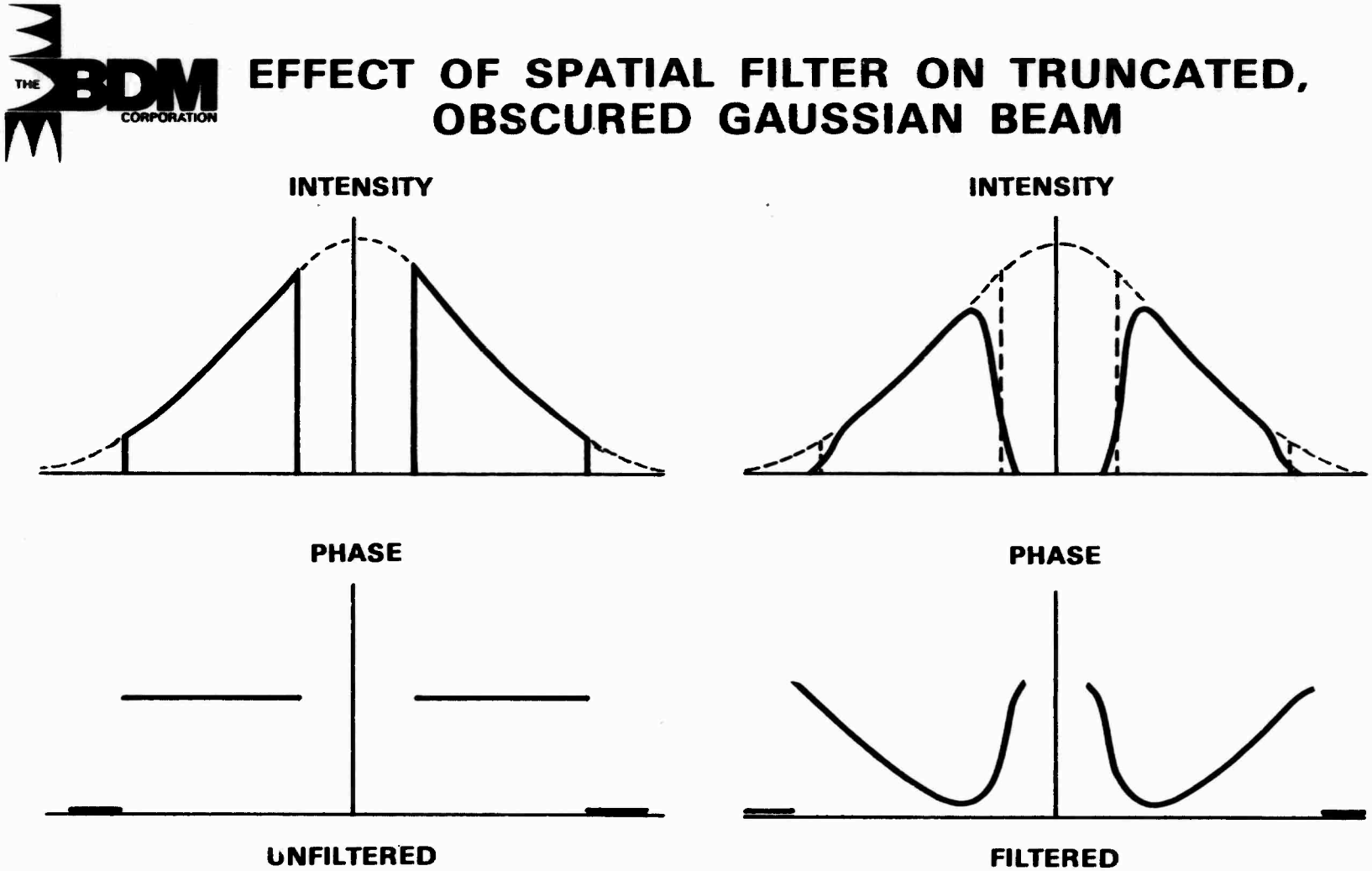

Figure 14. Spatial Filtering Modifies Both the Intensity and the Phase of Truncated, Obscured Gaussian Beam Profiles

THIS PAGE INTENTIONALLY LEFT BLANK.

THE LOTS CODE MODELS

Two HEL beam train physical optics codes were evaluated for use in this study: (1) the system optical quality (SOQ) code developed for the AFWL by Pratt and Whitney; and (2) the laser optical train simulation (LOTS) code developed for LASL by Dr. G. N. Lawrence while at the University of Arizona, Optical Sciences Center. Either code could have been used, but the LOTS code was chosen because it required less modification and was simpler to use.

A generic HEL beam train consisting of 10 high power mirrors plus the primary mirror was chosen as illustrated in figure 15. The total collimated beam length and Fresnel number (collimated) were chosen to be approximately 3000 cm and 300, respectively. The maximum baseline phase error (cumulative for all 10 mirrors) was taken to be about 0.5 waves.

GENERIC HEL BEAM TRAIN

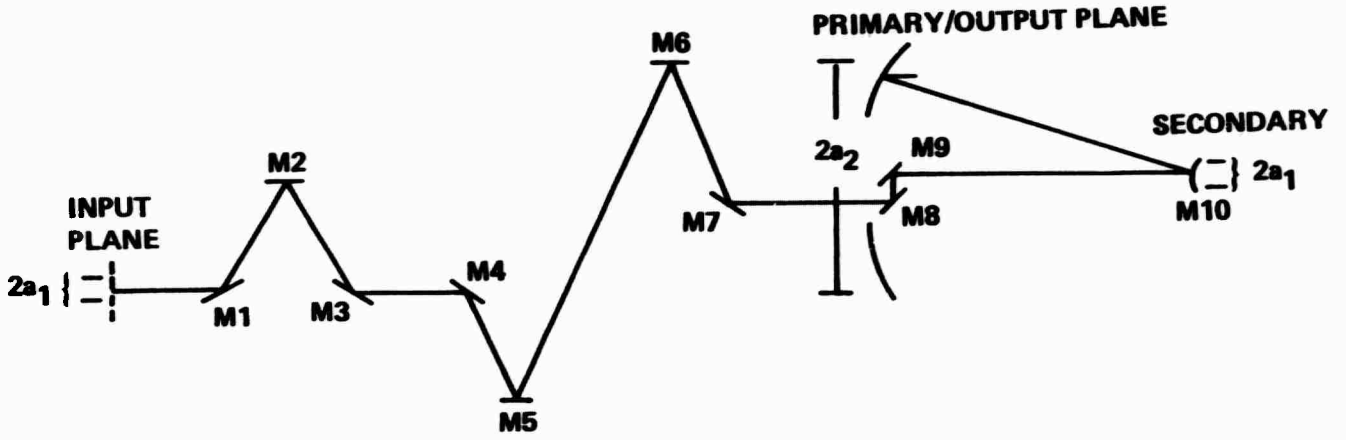

ASSUME:

1) 10 HI-POWER MIRRORS
2) COLLIMATED LENGTH ≈ 3000 cm
3) $F_N = a^2/\lambda L \approx 300$
4) REFLECTIVITY ≈ .998
5) THERMAL BOWING ≈ 0
6) FLUX DISTORTION ≈ 0.5 WAVES (MAX)

BDM/A-81-606-TR

Figure 15. Generic HEL Beam Train Model Developed for Spatial Filtering Effects Study

Because of the very high Fresnel number (~300) of the beam train, a lumped mirror element model was used to reduce computation time and lower overall costs. There were two justifications for this choice. The first, shown in figure 16, was that there is little error. The second was that the object was to determine the relative effect of the spatial filter as a point of principle as opposed to modeling its effect in a specific HEL beam train.

LUMPED VS. DISTRIBUTED MIRROR BEAM TRAIN THERMAL DISTORTION MODELS

	COMPARISON		
	DISTRIBUTED	LUMPED	% DIFFERENCE
STREHL (AT PRIMARY)	.93169	.88556	5
RELATIVE ENERGY (AT PRIMARY)	1.00000	.99890	.1
RELATIVE PEAK INTENSITY (IN FAR FIELD)	1.00000	.97010	3

CONCLUSION: BECAUSE HIGH FRESNEL NUMBERS CHARACTERIZE HEL BEAM TRAIN, A LUMPED ELEMENT MODEL MAY BE USED WITH LITTLE ERROR.

BDM/A-81-606-TR

Figure 16. Comparison Between Distributed and Lumped Mirror Element Beam Train Models

The original approach was to filter the beam immediately upon entering the beam train (model A), then apply a phase aberration to represent the effect of flux dependent thermal mirror distortion for all 10 mirrors at once, propagate the beam up to the secondary mirror, perform simple focus correction to the beam phase (removing as much phase error as possible), expand the beam through the telescope, and, finally, propagate it to the far field.

After finding that the results of spatial filtering on performance were negative for the characteristic input beam for model A, model B was set up and investigated. Results of model B confirmed that the change in beam shape and phase caused by the spatial filter was the cause of the behavior observed in figure 6. (See figure 17.)

TWO DIFFERENT LOCATIONS OF THE SPATIAL FILTER IN THE BEAM TRAIN WERE EXAMINED

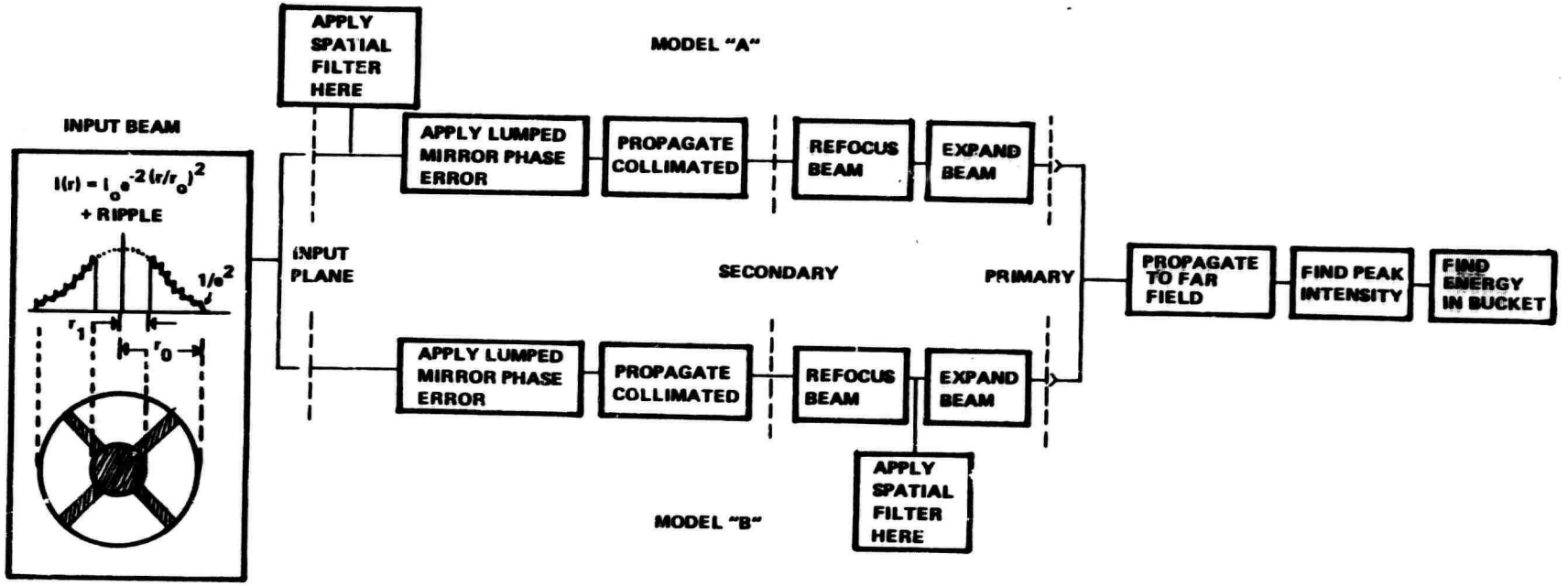

BDM/A-81-605-TR

Figure 17. Block Diagram of the Lumped Element Generic HEL Beam Train Model for Two Different Locations of the Spatial Filter

The steps illustrated in figure 18 initialize and save the starting nonuniform intensity distribution - a truncated Gaussian with central and radial obscurations and an added spatial frequency component.

LOTS CODE REQUIRED TO INITIALIZE A TYPICAL NONUNIFORM INTENSITY DISTRIBUTION WITH ADDITIONAL SPATIAL FREQUENCY COMPONENTS

```
100=C INITIALIZE GAUSSIAN BEAM
110=C WITH INNER OBSCURATION AND OUTER TRUNCATION
120=C WITH STRUT OBSCURATION
130=C WITH ADDED SPATIAL FREQUENCY
140=C
150=UNITS .6
160=LAMDA 2.7
170=APOD 15 25513
180=CLAP 15
190=RIPPLE .1 8.1522
200=GOOBS
210=   29.   30.
220=  -30.  -29.
230=  -29.  -30.
240=   30.   29.
250=GOOBS
260=   30.  -29.
270=  -29.   30.
280=  -30.   29.
290=   29.  -30.
300=GOBS 5
310=CLAP 15
320=PR64
330=STATION
340=INITIAL DISTRIBUTION
350=PROFILE 1
360=ENERGY
370=OUTPUT 1
380=EXIT
++
```

GENERATE TRUNCATED GAUSSIAN

ADD SPATIAL FREQUENCY

APPLY RADIAL (STRUT) OBSCURATION

APPLY CENTRAL OBSCURATION

BDM/A-81-605-TR

Figure 18. LOTS Code Describing Initiation of a Truncated, Centrally Obscured Gaussian Beam with Radial (Strut) Obscurations and Added Spatial Frequency

Figure 19 shows the strut pattern imposed on the beam. The beam is circular.

CROSSECTIONAL VIEW OF INITIAL INTENSITY DISTRIBUTION SHOWING RADIAL STRUT OBSCURATIONS

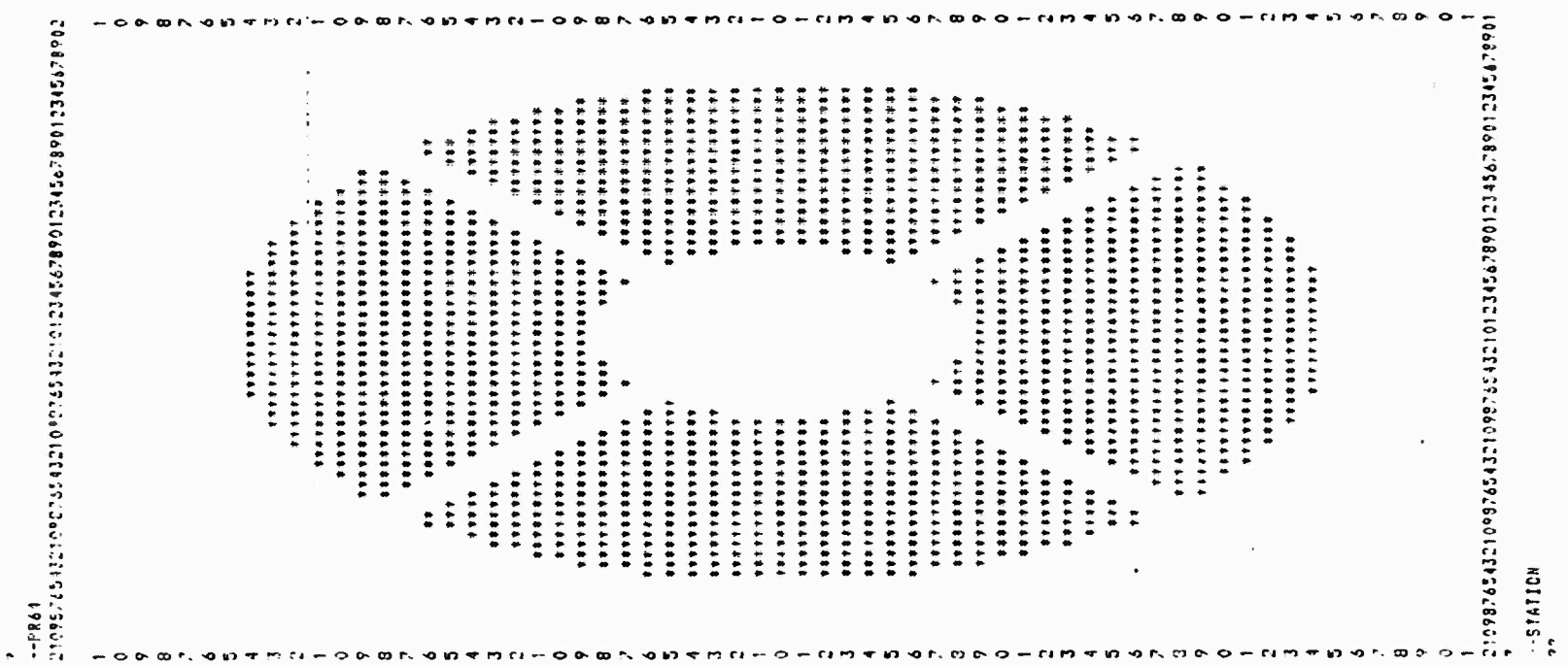

BDM/A-81-605-TR

Figure 19. Cross Section of Gaussian Beam Profile Generated by LOTS Code Showing Truncation, Central Obscuration, and Strut (Radial) Obscuration (Beam is Circular)

The complete listings of all steps required to model the generic beam train models (A and B) using the LOTS code are shown in figure 20. These models were very easy to set up, debug, modify, and run using LOTS. All results including plots were obtained running interactively from a remote terminal.

LOTS CODE FOR GENERIC HEL BEAM TRAIN MODEL — MODEL A: APPLY SPATIAL FILTER FIRST; MODEL B: APPLY FILTER AT SECONDARY OF BEAM EXPANDER

MODEL A

APPLY SPATIAL FILTER

APPLY THERMAL DISTORTION

PROPAGATE

REFOCUS BEAM

EXPAND BEAM

PROPAGATE TO FAR FIELD

```
100=C GENERIC LUMPED ELEMENT OPTICAL TRAIN
110=C
120=C STANDARD INPUT DISTRIBUTION
130= C TRUNCATED,OBSCURATED GAUSSIAN
140=BUFFER 1
150=STATION
160=FOCUS THE BEAM
170=IMAGE 200
180=C REFRAC SPATIAL FILTER
190=ENERGY
200=ISHORT
210=CLAP .0066
220=C AFTER SPATIAL FILTER
230=ENERGY
240=ISHORT
250=C RECOLLIMATE THE BEAM
260=PUPIL 200
270=CLAP 15
280=STATION
290=AFTER RECOLLIMATION
300=ENERGY
310=STREHL
320=PROFILE 1
330=STATION
340=APPLY LUMPED MIRROR PHASE ERROR
350=INTPHAS 2.222E-5
360=STATION
370=AFTER INTPHASE
380=STREHL
390=PROFILE 1
400=DIST 2700
410=STATION
420=AT SECONDARY
430=STREHL
440=PROFILE 1
450=REFOCUS
460=ENERGY
470=STATION
480=AFTER FOCUS CORRECTION
490=STREHL
500=PROFILE 1
510=GAUSTP 0. 1. 30. 400. -467.
520=ENERGY
530=CLAP 200
540=STATION
550=PRIMARY MIRROR OUTPUT BEAM
560=ENERGY
570=STREHL
580=IMAGE 1.E+00
590=STATION
600=FAR FIELD BEAM
610=ENERGY
620=RELPK
630=ENERGY
640=ENERGY
650=CLAP 82.35
660=C ENERGY IN 1 BIRY RADIUS
670=ENERGY
680=IMGPLOT
690=STRPLOT
700=END
```

MODEL B

APPLY THERMAL DISTORTION

PROPAGATE

REFOCUS BEAM

APPLY SPATIAL FILTER

EXPAND BEAM

PROPAGATE TO FAR FIELD

```
100=C GENERIC LUMPED ELEMENT OPTICAL TRAIN
110=C
120=C STANDARD INPUT DISTRIBUTION
130= C TRUNCATED,OBSCURATED GAUSSIAN
140=BUFFER 1
150=STATION
160=APPLY LUMPED MIRROR PHASE ERROR
170=INTPHAS 2.222E-5
180=STAT 20
190=AFTER INTPHASE
200=STREHL
210=PROFILE 1
220=DIST 2700
230=STATION
240=AT SECONDARY
250=STREHL
260=PROFILE 1
270=FOCUS .4
280=REFOCUS
290=ENERGY
300=STATION
310=AFTER FOCUS CORRECTION
320=STREHL
330=PROFILE 1
340=STATION
350=FOCUS THE BEAM
360=IMAGE 200
370=C REFRAC SPATIAL FILTER
380=ENERGY
390=ISHORT
400=CLAP .004
410=E AFTER SPATIAL FILTER
420=ENERGY
430=ISHORT
440=C RECOLLIMATE THE BEAM
450=PUPIL 200
460=CLAP 15
470=STATION
480=AFTER RECOLLIMATION
490=ENERGY
500=STREHL
510=PROFILE 1
520=GAUSTP 0. 1. 30. 400. -467.
530=ENERGY
540=CLAP 200
550=STATION
560=PRIMARY MIRROR OUTPUT BEAM
570=ENERGY
580=STREHL
590=IMAGE 1.E+00
600=STATION
610=FAR FIELD BEAM
620=ENERGY
630=RELPK
640=ENERGY
650=ENETRC
660=CLAP 82.35
670=C ENERGY IN 1 AIRY RADIUS
680=ENERGY
690=IMGPLOT
700=STRPLOT
710=END
```

BDM/A-81-606-TR

Figure 20. LOTS Code for the Two HEL Generic Beam Train Models

Figure 21 shows a starting intensity and phase distribution for the case where a 3.0 cm periodic ripple at 10 percent of peak intensity has been added to the beam. The ripple results in a spatial frequency component centered about .333 cycles/cm in the frequency domain.

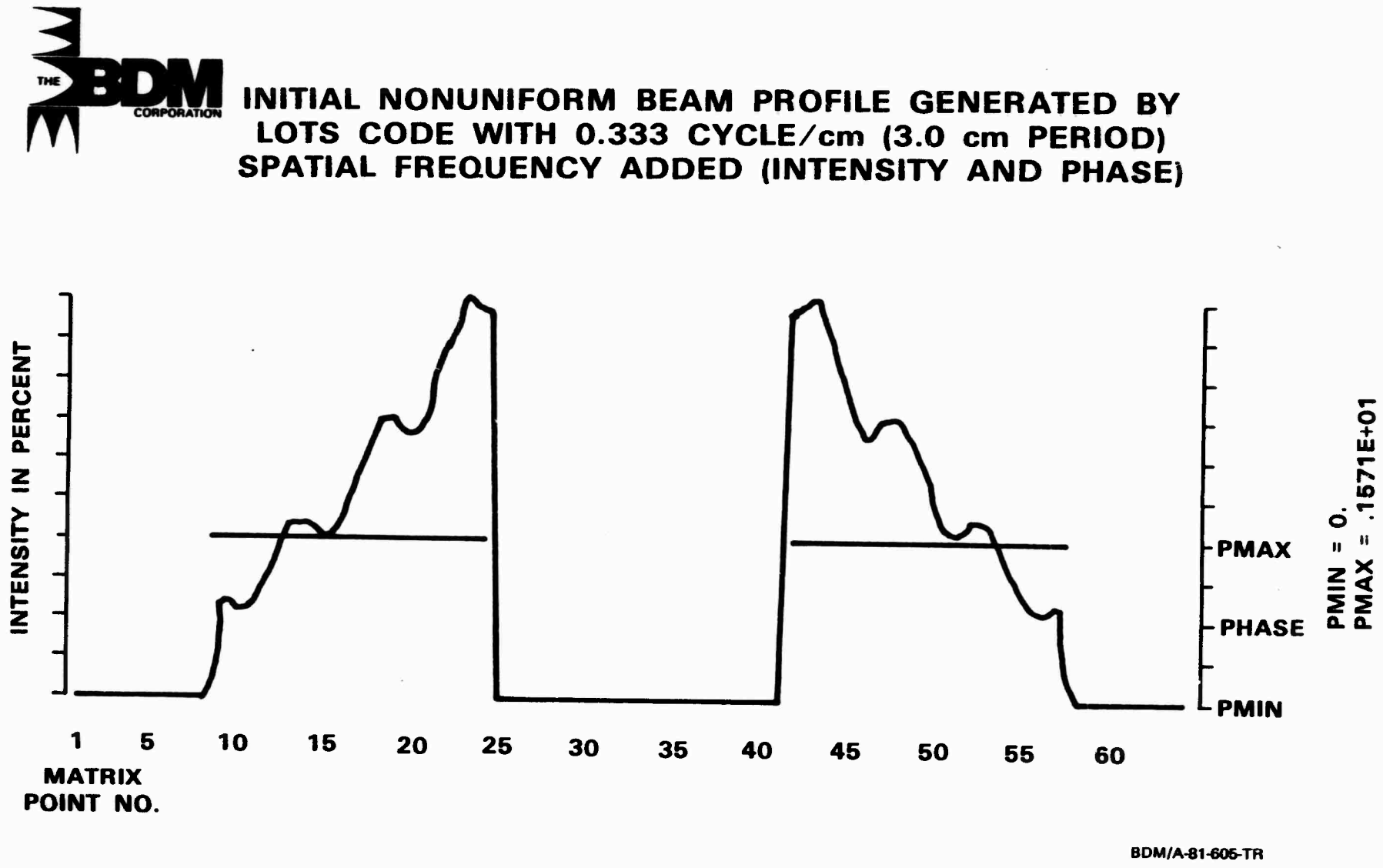

Figure 21. Starting Intensity and Phase Profiles Generated By LOTS Code for a 3.0 cm Period Added Ripple Component

Figure 22 shows the starting distribution which results in an added spatial frequency component centered about 0.544 cycles/cm in the frequency domain. This was the highest spatial frequency which could be examined with the present version of the LOTS code.

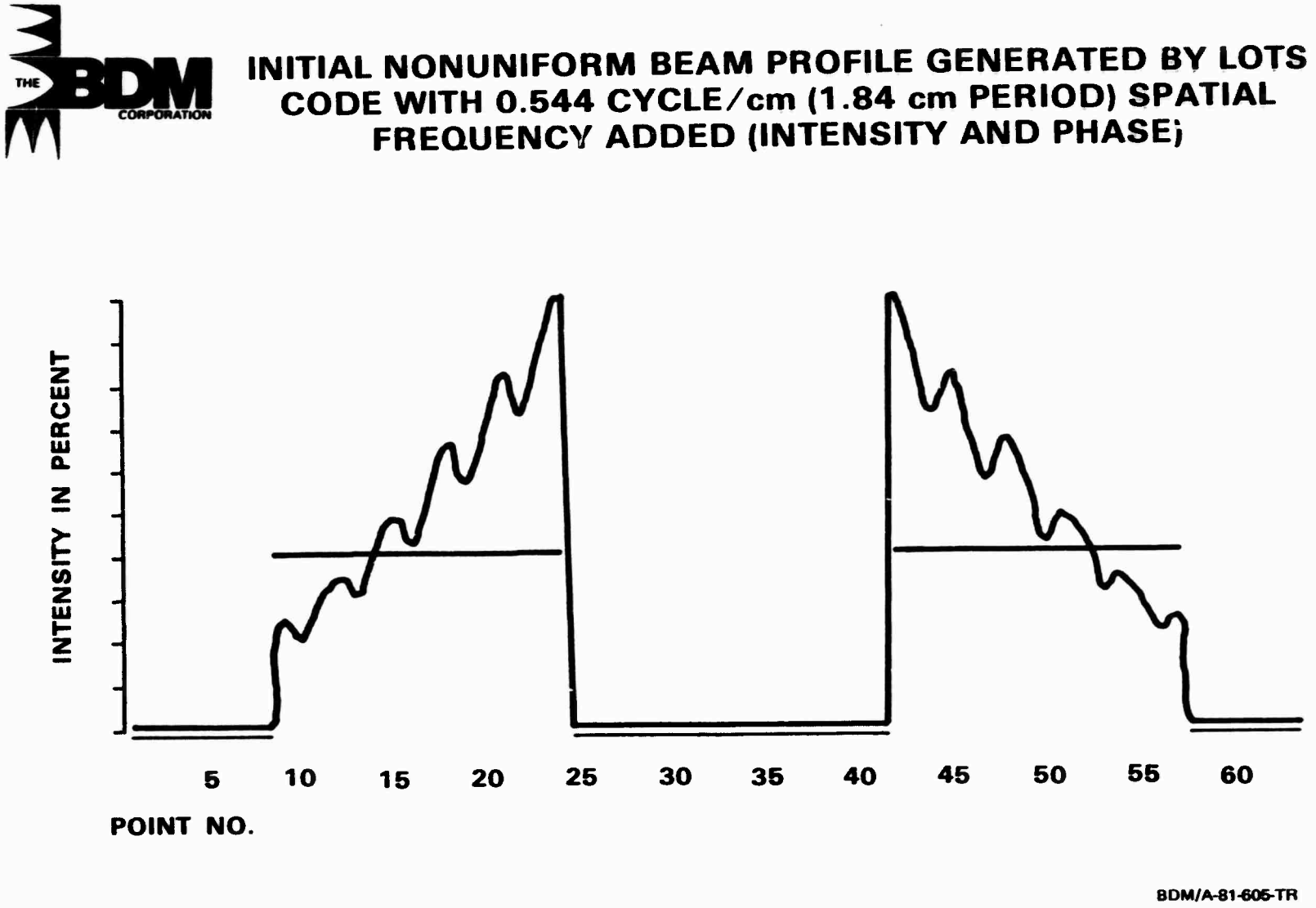

Figure 22. Starting Intensity and Phase Profiles Generated by LOTS Code for a 1.84 cm Period Added Ripple Component

Part of the first study objective (figure 3) was to establish the impacts of the truncated, obscured Gaussion intensity with added high spatial frequency on baseline performance, i.e. to establish baseline performance in terms of the amount of phase aberrations resulting from flux dependent mirror distortion and of far field performance. These results are summarized in figure 23 and in the next several pages.

IMPACTS OF NONUNIFORM INTENSITY DISTRIBUTION* ON BASELINE PERFORMANCE — NO SPATIAL FILTERING

IMPACT OF NONUNIFORM INTENSITY DISTRIBUTION ON MIRROR DISTORTION:

- ADDS MAXIMUM OF 0.54 WAVES OF PHASE ERROR; SIMPLE FOCUS CORRECTION REMOVES 0.46 WAVES
- GENERALLY GETS WORSE WITH SPATIAL FILTERING (ESPECIALLY MODEL A)

IMPACT OF NONUNIFORM INTENSITY DISTRIBUTION ON FAR FIELD PERFORMANCE:

- PERFORMANCE GENERALLY WORSENS AS SPATIAL FREQUENCY INCREASES

---

*TRUNCATED GAUSSIAN WITH CENTRAL AND RADIAL OBSCURATIONS AND AN ADDED SPATIAL FREQUENCY COMPONENT

BDM/A-81-605-TR

Figure 23. Impacts of Nonuniform Intensity Distribution on Baseline Performance (Performance in the Absence of Spatial Filtering)

Figure 24 summarizes the essential details of the flux distortion model used to apply phase errors to the beam. This number, expressed in waves of distortion as $\frac{\Delta\Phi}{2\pi}$, varies across the beam front. Points of higher flux result in greater amounts of wave distortion. The maximum amount of wave distortion added in this study from mirror distortion for all cases examined was not greater than 0.7 waves when considered as a function of spatial filter radius (recall that the filter modified the intensity and phase of the initial distribution (model A) - this makes thermal distortion become dependent of the spatial filter radius).

FLUX DISTORTION MODEL

$\Delta\phi(x, y) = 2\pi\alpha I(x, y)$

$\alpha = \frac{2\ DISTF\ (1 - R)}{\lambda}$ (waves/watt/cm²)

DISTF = FLUX DISTORTION FACTOR (cm/watt/cm²)

R = MIRROR REFLECTIVITY

λ = WAVELENGTH (cm)

$\frac{\Delta\phi}{2\pi} \leq 0.7$ wave

BDM/A-81-606-TR

Figure 24. The Thermal Flux Distortion Mirror Model

Before examining the impact of the representative nonuniform intensity distribution on mirror distortion, it is instructive to consider the mirror distortion phase error which results from an untruncated, unobscured Gaussion beam distribution containing 10 percent added spatial frequency at 0.544 cycles/cm. This is shown in figure 25 as a function of spatial filter radius. Baseline impact is given for a spatial filter radius of 0.064 cm. The dotted curve is the amount of maximum phase error (in units of $\frac{\Delta\Phi}{2\pi}$ waves) across the entire beam phase front which resulted from thermal distortion and which was added to the beam phase prior to the collimated propagation (model A, step INTPHAS, figure 20). Because of earlier comments, this phase error is a function of the spatial filter radius. The dashed curve in figure 25 is the amount of phase error removed at the secondary by allowing only focus correction. The solid curve (read right abscissa) is the percent residual phase distortion remaining after focus correction (i.e. the difference of the dotted and dashed curves expressed as a percentage of the error added). These results indicate that the filter does improve the effect of mirror distortion phase error resulting from a high spatial frequency. The solid curve correlates well with the upper set of curves in figure 11.

IMPACT OF AN UNTRUNCATED, UNOBSCURED GAUSSIAN INTENSITY DISTRIBUTION ON MIRROR DISTORTION (MODEL A)

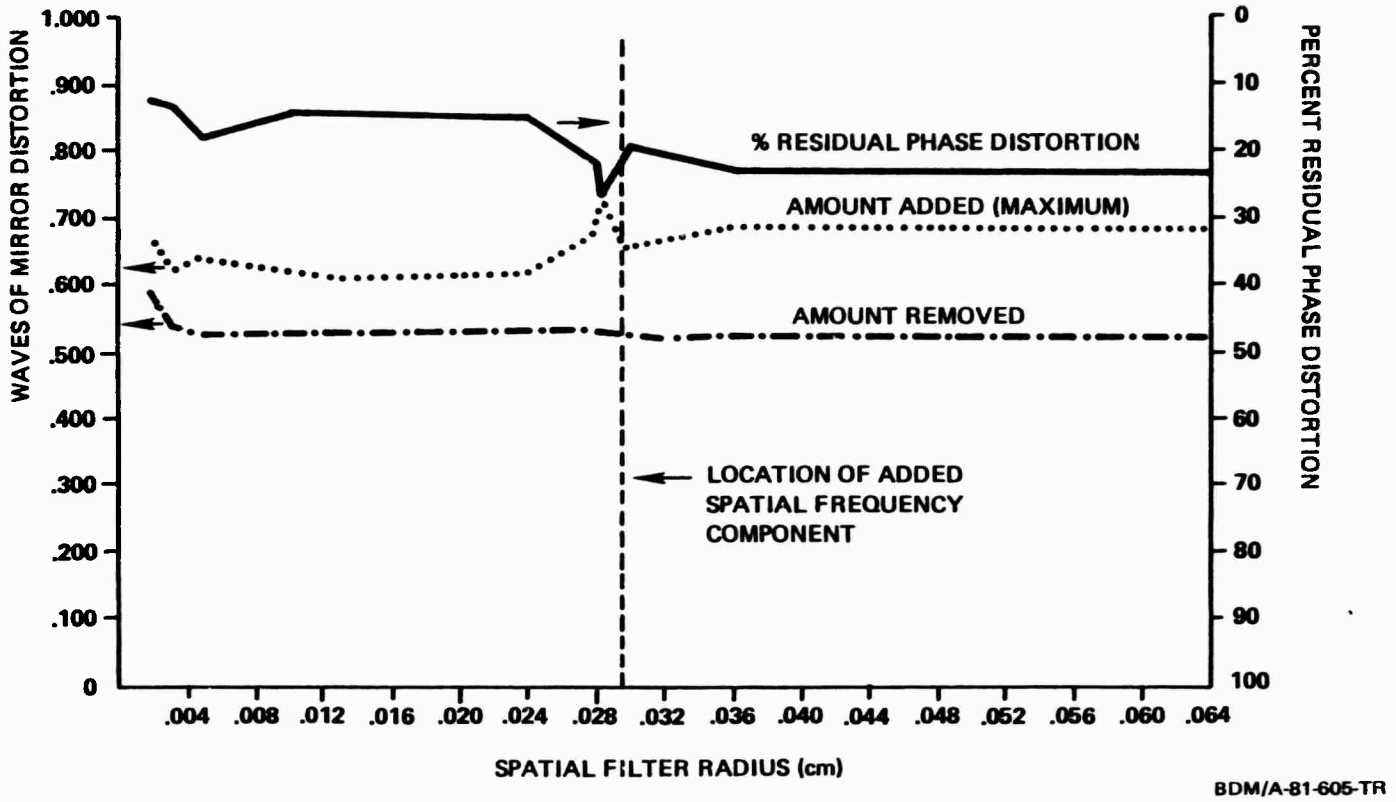

Figure 25. Impact of Untruncated, Unobscured Gaussian Beam Distribution on Mirror Distortion (0.544 cycles/cm data) (Model A)

The meanings of the curves in figure 26 are the same as in figure 25. Baseline performance impact is given for a filter radius of .064 cm. The solid curve in figure 26 says that the amount of residual phase error generally increases as the filter radius decreases (increasing filtering) for the case of thermal distortion phase errors resulting from spatially filtered truncated, obscured Gaussian intensity profiles with added 0.544 cycle/cm spatial frequency. However, at very small (.002 cm) filter radii there is a dramatic decrease in residual phase error. As already mentioned, the beam has been so severely filtered that all sharp edges have been completely rounded and obscurations filled: it is now, in effect, a purely Gaussian beam profile. The phase error for such a distortion is effectively characterized by thermal bowing which is easily correctable with simple focus correction, hence the small residual phase error. Also note the good correlation between the solid curve in figure 26 and the lower set of curves in figure 11.

IMPACT OF NONUNIFORM* INTENSITY DISTRIBUTION ON MIRROR DISTORTION (MODEL A)

*TRUNCATED, OBSCURED GAUSSIAN BEAM WITH 10% ADDED SPATIAL FREQUENCY AT 0.544 CYCLES/cm FILTERED BEFORE APPLYING MIRROR DISTORTION

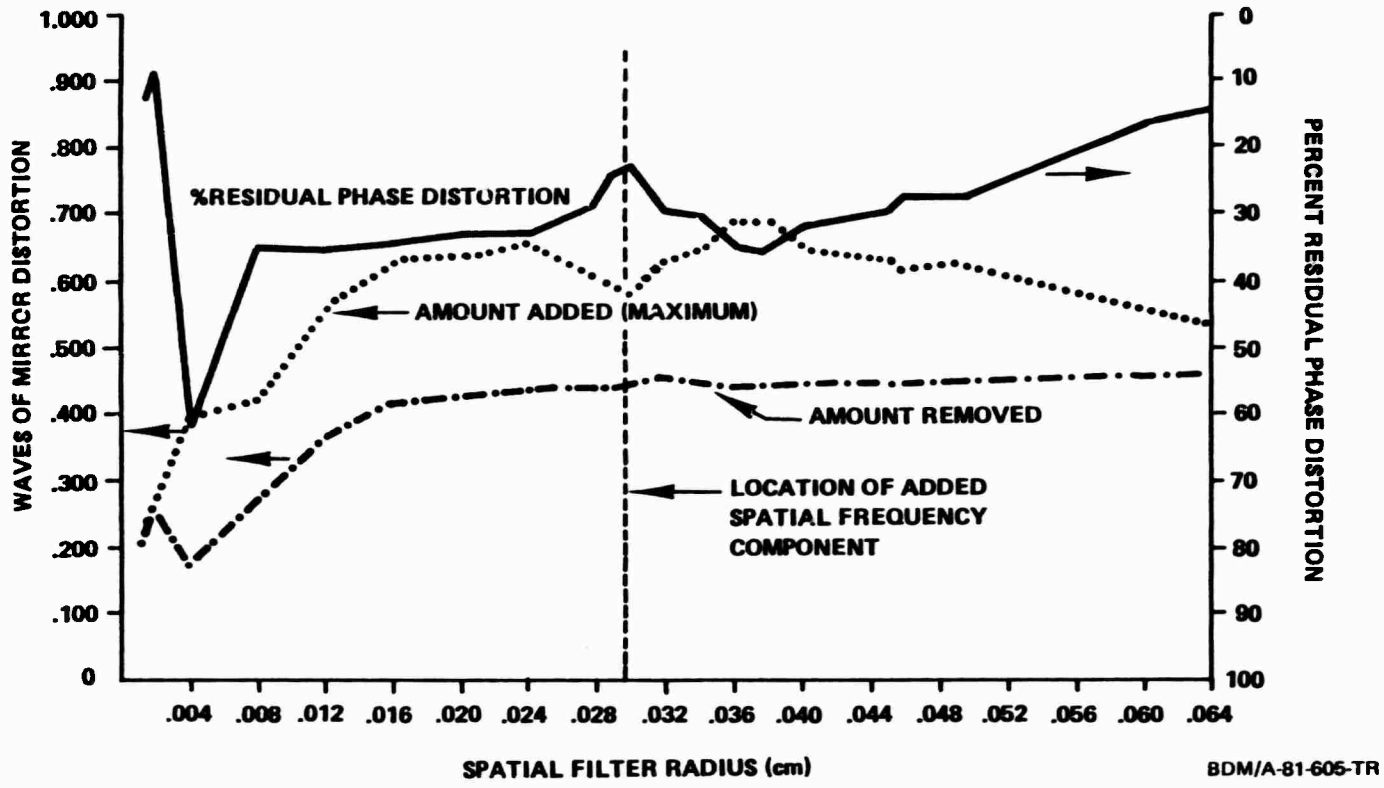

Figure 26. Impact of a Truncated, Obscured Gaussian Beam Distribution on Mirror Distortion Phase Errors (0.544 cycle/cm data) (Model A)

Figure 27 shows the impact of the truncated, obscured Gaussian beam profile with .544 cycle/cm ripple on mirror distortion phase error for the case of model B (see figures 17 and 20). Because the spatial filter is not applied until after the beam reaches the secondary, the amount of mirror distortion phase error is independent of the spatial file.

IMPACT OF NONUNIFORM INTENSITY DISTRIBUTION* ON MIRROR DISTORTION (MODEL A)

*TRUNCATED, OBSCURED GAUSSIAN BEAM WITH 10% ADDED SPATIAL FREQUENCY AT 0.544 CYCLES/cm FILTERED AFTER APPLICATION AND CORRECTION OF MIRROR DISTORTION

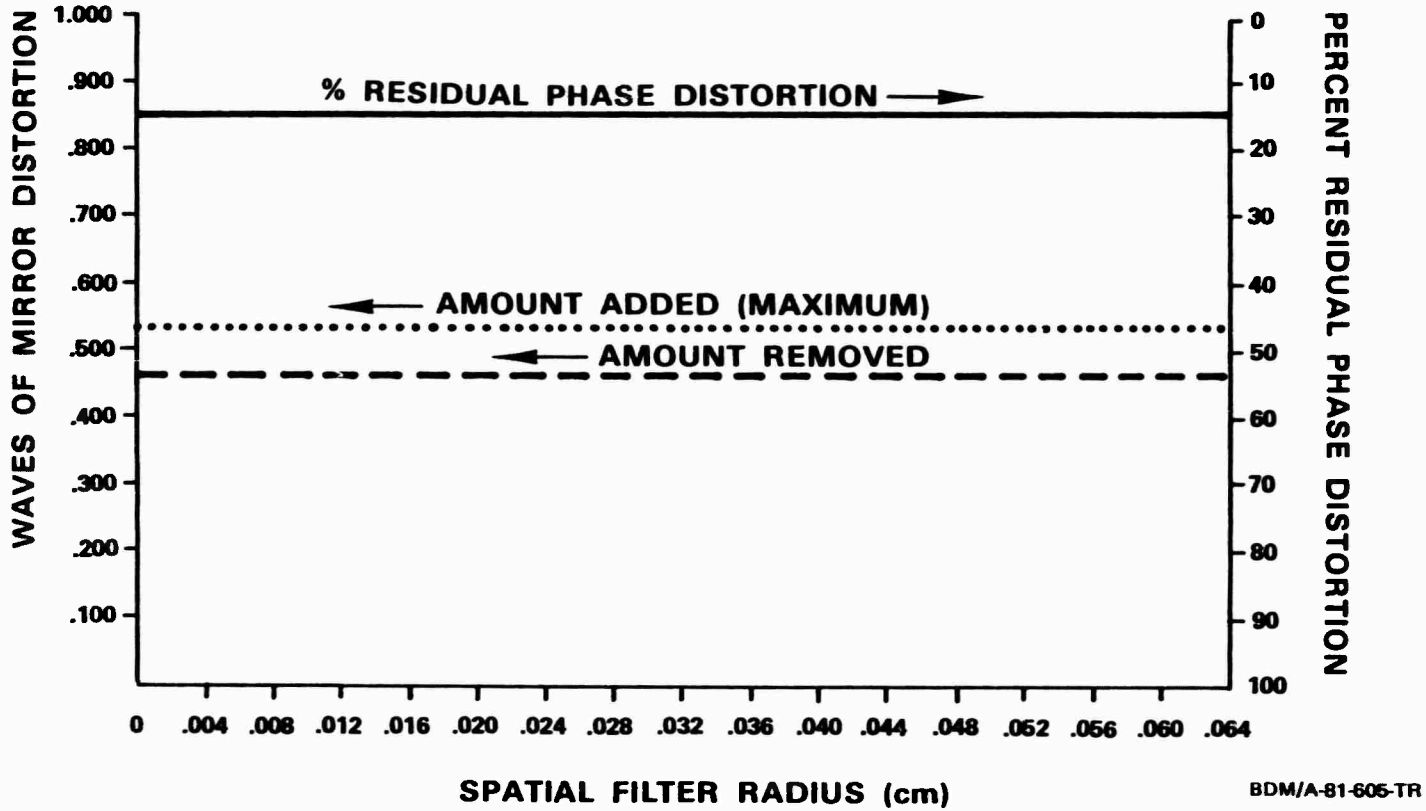

Figure 27. Impact of Truncated, Obscured Gaussian Beam Distribution on Mirror Distortion Phase Errors (0.544 cycle/cm data) (Model B)

When the spatial filter radius is large enough that it has no effect (radius $\geq$ 0.064 cm), the baseline far field performance for this generic HEL beam train propagating truncated, obscured Gaussian beams for several different added spatial frequencies is summarized in figure 28. Zero frequency peak intensity has been arbitrarily set to unity. From the data it is seen that baseline performance in the far field should degrade as spatial frequency of beam nonuniformities increases.

IMPACT OF NONUNIFORM INTENSITY DISTRIBUTIONS* ON FAR FIELD PERFORMANCE — NO FILTERING

*TRUNCATED GAUSSIAN WITH CENTRAL AND RADIAL OBSCURATIONS AND ADDED SPATIAL FREQUENCY COMPONENTS

SPATIAL FREQUENCY ADDED[1] (CYCLES/cm)	PHASE ERROR ADDED (WAVES)	PHASE ERROR REMOVED (WAVES)	STREHL (AT PRIMARY)	RELATIVE PEAK INTENSITY[2]	POWER IN AIRY SPOT[3] (%)
0	.496	.476	.88556	1.00	59.2
.3333	.499	.448	.86356	.97	56.8
.5435	.509	.437	.87007	.97	56.6

(1) AT 10% OF PEAK AMPLITUDE

(2) IN FAR FIELD

(3) POWER INSIDE SPOT OF RADIUS = 0.61 $R\lambda/D$

BDM/A-81-606-TR

Figure 28. Impact of a Truncated, Obscured Gaussian Beam on Far Field Performance as a Function of Different Spatial Frequency Errors

Objective 3 (of figure 3) involves the geometrical design of a spatial filter for suitable use in a HEL beam train. A cylindrical filter (i.e. one where M1 in figure 2 has concave curvature only one transverse axis) produces a line focus. The peak flux loads on such a filter will be much lower than those on a circular aperture filter using point focusing optics. The key parameters required to design the geometry of the cylindrical spatial filter are summarized in figure 29. The objective of the design is to find the peak flux load on the spatial filter as functions of pupil intensity I (e.g. intensity at M1 in figure 2) and the edge of the spatial filter X_{SF}.

CYLINDRICAL SPATIAL FILTER PARAMETERS

ASSUME A LINE IMAGE AND A UNIFORMLY FILLED RECTANGULAR APERTURE

- a = APERTURE WIDTH = 30 cm
- λ = WAVELENGTH = .00027 cm
- F = FOCAL LENGTH OF CYLINDRICAL LENS = 200 cm
- I_o = UNIFORM FLUX = w/cm^2
- fc = CUTOFF FREQUENCY OF SPATIAL FILTER = 6/a
- X = DISTANCE FROM CENTER OF SPATIAL FILTER
- X_{SF} = LOCATION OF EDGE OF SPATIAL FILTER

ASSUME FLUX OVER 30 x 30 cm RECTANGULAR APERTURE IS

I_o = w/cm^2

BDM/A-81-605-TR

Figure 29. Cylindrical Spatial Filter Parameters

Figure 30 shows the intensity distribution across a line focus produced by a cylindrical mirror. For a cutoff frequency of $fc = \frac{6}{a}$, where a is the width of the cylindrical mirror (at M1 in figure 2), the location of the edge of the spatial filter aperture X_c is known. The intensity resulting at X_c is approximately $47I_o$ for the cutoff frequency chosen. Relative to the high spatial frequency components considered in this report and realistic HEL beam duct sizes of interest, this cutoff frequency would be quite low. Since peak flux loads on the spatial filter will increase as the cutoff frequency decreases, the value calculated here should probably be considered worst case.

NOMINAL FLUX ON CYLINDRICAL SPATIAL FILTER

CYLINDRICAL IMAGE DISTRIBUTION

$$I(x) = I_o \frac{a^2}{\lambda F} \frac{\text{SIN}^2\left(\frac{\pi a x}{\lambda F}\right)}{\left(\frac{\pi a x}{\lambda F}\right)^2}$$

$$\sim I_o \frac{\lambda F}{\pi^2 x^2} \text{ , FOR } x > \frac{a}{\lambda F}$$

(i.e., AWAY FROM IMAGE CENTER)

FOR CUTOFF FREQUENCY OF $f_c = 6/a$

$$f_c = \frac{X_c}{\lambda F} = \frac{6}{a}$$

$$X_c = \frac{6\lambda F}{a}$$

$$I(X_c) = I_o \frac{a^2}{36\pi^2 \lambda F} \approx 47\, I_o$$

BDM/A-81-605-TR

Figure 30. Nominal Flux Loads on a Cylindrical Spatial Filter

Figure 31 summarizes the results of geometrical and material analyses for the cylindrical spatial filter. (The materials analysis follows.) The absorption of power deposited on the filter depends on the material. Best estimates for multi-layer dielectric coatings $(Si,SiO_x)^n Ag$ on molybdanum or silicon substrates give $\alpha = .001$. This would result in an absorbed power by the filter of $\alpha(47I_o)$ watts/cm^2. Initial estimates of damage thresholds for a filter made of this material could be as high as 250 joules/cm^2 (for 0.1 μsec pulses). It is believed, based on these results, that absorbed power by a spatial filter will not be a factor limiting or precluding its use in a HEL beam train.

CYLINDRICAL FILTER ABSORBED POWER

BEST ESTIMATE OF NOMINAL SPATIAL FILTER ABSORPTION IS*

$$\alpha = .001$$

ABSORBED POWER = $\alpha(47\ I_o)$ **(watts/cm²)**

INITIAL ESTIMATE OF SPATIAL FILTER DAMAGE THRESHOLD FOR 0.1 μsec PULSES IS*

180 - 250 (J/cm²)

***SEE RESULTS OF SPATIAL FILTER MATERIAL DESIGN STUDY (FOLLOWING)**

BDM/A-81-606-TR

Figure 31. Power Absorbed on a Cylindrical Spatial Filter Versus Damage Threshold

The fourth objective of this effort (figure 3) addresses materials for possible use as a spatial filter in a space-based, high energy HF/DF laser system. The attempt is to identify the most promising candidate materials in terms of lowest optical absorptions and highest damage thresholds. Since cooling studies were not performed, no conclusions are drawn here regarding the actual viability of such a filter.

A survivable material spatial filter must satisfy two criteria: (1) it must have the lowest possible absorption to meet power handling requirements; and (2) it must withstand the space radiation (particle, x-ray, and UV) environment without degrading below acceptable limits. (See figure 32.)

The obvious "first cut" design for such a filter is to utilize a highly enhanced reflective (ER) mirror having the appropriate aperture (circular or line) to accomplish clean-up of higher order spatial modes. Multilayer dielectric (MLD) coated filter surfaces will present low absorption losses to the HEL beam. However, an uncoated filter, or one with a sputtered metal layer coating may have a higher catastrophic damage threshold, particularly if damage in the structure is coating limited. In either case, the starting surface must be carefully prepared (e.g. diamond turned and inclusion free) to achieve maximum threshold values.

HF SPATIAL FILTER DESIGN GUIDELINES

CRITERIA FOR SURVIVABLE SPATIAL FILTER

(1) LOW ABSORPTION TO MEET POWER HANDLING REQUIREMENTS IN THE LASER ENVIRONMENT

(2) NEGLIGIBLE DEGRADATION IN ABSORPTION IN THE SPACE RADIATION ENVIRONMENT (PARTICLE, X-RAY, UV)

APPROACH — COMPARE DAMAGE THRESHOLDS BETWEEN MULTILAYER DIELECTRIC COATED SUBSTRATES AND UNCOATED, OR SPUTTERED METAL LAYER COATED, SUBSTRATES.

STUDY LIMITATIONS — NO COOLING STUDIES PERFORMED

BDM/A-81-605-TR

Figure 32. HF/DF Spatial Filter Material Design Guidelines

In general, higher damage thresholds at 2.7 and 3.8 μm (see figure 33) have been achieved in uncoated diamond turned copper[1,4] (~ 180-195 J/cm^2 for 0.1 μsec pulses). However, some advanced coating designs have achieved damage thresholds as high as 150 J/cm^2 which is close to the uncoated values[1]. The possibility clearly exists for greatly increasing these thresholds by improving coating deposition technology. Therefore, we will focus the remainder of this discussion on advanced coated spatial filter designs.

Excellent treatments of advanced (ER) coatings for HF/DF laser wavelengths have been given by Donovan, et al.[1,5] They considered both absorption and space environment-induced degradation effects on coated Mo mirrors. It should be emphasized that filters coated with the conventional $(ZnS, ThF_4)^n$ Ag layers on Mo substrates are unsatisfactory for space applications. While these designs may perform well under laser irradiation, they degrade rapidly when subjected to short term solar UV, electron, and proton radiation.[3] An order of magnitude charge in 2.7μm absorption (along with visible discoloration) has been observed after exposures of 1000 equivalent solar hours (ESH).[1] Similar effects are observed for coated Ag/Mo substrates which use TlI/PbF_2 or As_2Se_3/NaF materials. However, advanced coatings of $(Si,Al_2O_3)^2Ag$ and $(Si,SiO_x)^4Ag$ are found to be stable in a space radiation environment. In addition, reflectivities as high as 0.9992 (absorptions of 8×10^{-4}) are achievable at HF wavelengths with Al_2O_3 and silicon pair designs.[1,3] In some cases, absorption actually decreases significantly with solar irradiation dose possibly due to UV induced absorption of impurities.[5] This presolar irradiation treatment can lead to increased laser damage thresholds. In addition, absorption of these coatings is also relatively stable with temperature from room temperature to about 200° C.

Pulsed HF damage testing of $(Si,Al_2O_3)^2$ Ag coated silicon mirrors have shown damage thresholds of 150-160 J/Cm^2; UV preirradiation can increase this value to as high as 250 J/Cm^2.[5]

2.7 AND 3.8 μm LASER DAMAGE THRESHOLDS

SPATIAL FILTER TYPE	DAMAGE THRESHOLD (0.1 μsec PULSES) (J/cm^2)
UNCOATED DIAMOND TURNED COPPER	180 - 195[1]
$(Si,AL_2O_3)^2$ Ag COATED SILICON	150 - 160[2]
UV PREIONIZED $(Si,AL_2O_3)^2$ Ag COATED SILICON	250[2]

[1] T. M. DONOVAN, et. al., PROCEEDINGS OF THE 1980 LASER INDUCED DAMAGE IN OPTICAL MATERIALS, NATIONAL BUREAU OF STANDARDS, BOULDER, COLORADO

[2] T. M. DONOVAN, et. al., PROCEEDINGS OF HIGH POWER LASER COMPONENTS MEETING, NOVEMBER 1-2, 1979, NWC TP6178, PART 1.

BDM/A-81-605-TR

Figure 33. HF/DF Laser Damage Thresholds in Some Materials

MAJOR REFERENCES USED FOR THIS MATERIALS STUDY

1. T. M. Donovan, T. O. Portens, S. C. Seitel, S. J. Holmes, and L. B. Fogdall, Enhanced Reflectance Mirrors for Space Borne HF Laser Applications, in Proc. of the 1980 Laser Induced Damage in Optical Materials, National Bureau of Standards, Boulder, Colo.

2 S. J. Holmes, "Multilayer Enhanced Reflectors for the HF Laser Wavelength Region," Research & Technology Center, Final Technical Report on NWC Contract NG0530-79-C-0264 (1980).

3. L. B. Fogdall, et al., "Natural and Induced Space Radiation Effects on Optical Coatings and Materials," Boerrey Radiation Effects Laboratory. Final Report on NWC Contracts N00123-78-0989 and N60530-79-C-0263 (Dec. 1979).

4. J. O. Porteus, et al., "Dependancy of Metal Mirror Damage Thresholds on Wavelength, Material, Pulse Length, and Preparation Method." In 12th Annual Symposium on Optical Materials for High Power Lasers, Boulder, Colo., (1980).

5. T. M. Donovan et al., "Improvement of Laser Damage Resistance in Certain Enhanced Reflectance Mirror Designs Via Simulated Space Radiation" in Proc. of High Power Laser Components Meeting, 1-2 Nov. 1979, NWC TP 6178, Part 1.

CANDIDATE 2.7 μm MLD COATING COMPARISON

MULTI-LAYER DIELECTRIC COATINGS	PERFORMANCE	
	LASER ENVIRONMENT	SPACE ENVIRONMENT
$(ZnS, ThF_4)^nAg$	SATISFACTORY(1)	UNSATISFACTORY(2)
TlI/PbF_2	SATISFACTORY(1)	UNSATISFACTORY(2)
As_2Se_3/NaF	SATISFACTORY(1)	UNSATISFACTORY(2)
$(Si, AL_2O_3)^2Ag$	SATISFACTORY(3)	SATISFACTORY(4)
$(Si,SiO_x)^4Ag$	SATISFACTORY(3)	SATISFACTORY(4)

(1) REFLECTIVITY = .998

(2) ORDER OF MAGNITUDE INCREASE IN 2.7 μm ABSORPTION AND DISCOLORATION AFTER 1000 EQUIVALENT SOLAR HOURS EXPOSURE

(3) REFLECTIVITY = .9992, STABLE OVER 25°C - 200°C

(4) ABSORPTION ACTUALLY DECREASES WITH SPACE ENVIRONMENT EXPOSURE

BDM/A-81-605-TR

Figure 34. Comparison of HF/DF MLD Coatings

In conclusion, then, an HF spatial filter design utilizing $(Si,SiO_x)^nAg$ or $(Si,Al_2O_3)^nAg$ coatings on Mo or Si substrates would present the best possibility for a spatial filter design. These coatings show high damage thresholds as well as high resistance to the solar radiation space environment. Further studies are required to fully understand the role of solar UV radiation in reducing absorption, and correspondingly, in increasing damage thresholds of these materials.

HF SPATIAL FILTER MATERIALS RECOMMENDATION

- AN HF SPATIAL FILTER DESIGN UTILIZING (Si, SiO_x)^{n}Ag OR (Si, AL_2O_3)^{n}Ag COATINGS ON Mo OR Si SUBSTRATES SHOULD PRESENT THE BEST POSSIBILITY HIGH, STABLE DAMAGE THRESHOLD IN BOTH LASER AND SPACE ENVIRONMENTS

- FURTHER STUDIES ARE REQUIRED TO FULLY UNDERSTAND THE ROLE OF SOLAR UV RADIATION IN REDUCING ABSORPTION, AND CORRESPONDINGLY, IN INCREASING DAMAGE THRESHOLDS IN THESE MATERIALS

BDM/A-81-606-TR

Figure 35. Spatial Filter Material Design Recommendation